MODELLING HYDRAULIC EFFECTS FOR VARIOUS POSITIONS OF VEGETATION PATCHES IN A MEANDERING RIVER

KLEIJER, J.

MASTER OF SCIENCE IN EARTH SCIENCES THESIS

October, Utrecht 2014

Utrecht University, Faculty of Geosciences

Modelling hydraulic effects for various positions
of vegetation patches in a meandering river

Kleijer, J.
Student number: 3953343

Supervisors:
Prof. Dr. M.G. Kleinhans
Dr. E.A. Addink
M. van Oorschot

Utrecht University
Faculty of Geosciences
Department of Physical Geography

Universiteit Utrecht

Final version, October 31, 2014

ABSTRACT

Meander dynamics create elegant vegetation patterns on the river floodplain. Vegetation on the floodplain is known as riparian vegetation. This vegetation redistributes flow to the main channel and the water sets up in the river reach. However, generic effects of the position of the vegetation patches are not identified and can have implications for river and floodplain management of meandering systems. This study aims to find the hydrodynamic responses of the positioning of vegetation patches. With depth-averaged hydrological modelling, the hydraulic response is quantified by implementing vegetative patches on the floodplain in an idealized meandering system. The hydrological conditions, the location and the vegetation type determine the blockage factor of flow. Varying the position of the patch sets up the water level several centimetres in the main channel and a reduction of 10's of percentages of flow velocity on the floodplain. Vegetation closer to the channel redirects more flow through the channel as well as more vegetation patches. Submerged vegetation close to the main channel redistributes less flow compared to larger vegetation stands. Furthermore, flow between the patches seems to interact and further obstruct the flow over the floodplain. River and floodplain managers should take these findings of the effect of the position into account for future planning in river restoration projects and accounting for flood protection.

INDEX

LIST OF FIGURES

LIST OF TABLES

LIST OF NOTATIONS

$A_{arc-low}$	Area within the arc with a decreased velocity relative to the control simulation	$[m^2]$
$A_{arc-tot}$	Total area within the arc	$[m^2]$
A_{veg}	Vegetated area on the floodplain	$[m^2]$
b	Degree of non-linearity of sediment transport	[-]
B_x	Blockage factor	[-]
C	Chézy friction coefficient	$[m^{0.5}s^{-1}]$
C_b	Bed Chézy resistance coefficient	$[m^{0.5}s^{-1}]$
C_D	Drag coefficient along vegetation stems	[-]
C_r	Representative resistance coefficient	[-]
d	Diameter of the stems	[m]
D_{50}	Median grain diameter	[m]
D_{ch}	Distance to the channel	[m]
$f(\theta)$	Magnitude of the transverse bed slope effect	$[m^{-1}]$
F_D	Drag force	$[Nm^{-2}]$
g	Gravitational acceleration on earth = 9.81	$[ms^{-2}]$
h	Vegetation height	[m]
H	Water depth	[m]
$\bar{H}$	Average water depth	[m]
H_0	Water depth of the control simulation	[m]
H_{ch}	Channel depth	[m]
H_{fl}	Floodplain height	[m]
H_{veg}	Water depth of a simulation with vegetation	[m]
HSI	Habitat Suitability Index	[-]
i	Water level slope	[-]
IP	Interaction parameter	[-]
J_s	Skewness coefficient	[-]
J_f	Flatness coefficient	[-]
m	Vegetation density	$[m^{-2}]$
n	Number of patches	[-]
n_m	Number of meander waves	[-]
n_s	Number of stems per square meter	$[m^{-2}]$
Q	Discharge	$[m^3s^{-1}]$
Q_{ch}	Discharge through the channel	$[m^3s^{-1}]$
Q_{fl}	Discharge over the floodplain	$[m^3s^{-1}]$
s	Streamwise coordinate	[m]
S	Sinuosity	[-]
$\bar{u}$	Mean velocity	$[ms^{-1}]$
u_c	Flow velocity inside submerged vegetation	$[ms^{-1}]$
u_u	Flow velocity above submerged vegetation	$[ms^{-1}]$
u_*	Shear velocity	$[ms^{-1}]$
U	Flow velocity	$[ms^{-1}]$
V_0	Sum of the x- and y-directional velocity of the control simulation	$[ms^{-1}]$
V_{veg}	Sum of the x- and y-directional velocity of a simulation with vegetation	$[ms^{-1}]$
w	Width of the vegetation patch	[m]
W	Channel width	[m]
W_{ch}	Channel width	[m]
W_{fl}	Mean floodplain width	[m]
z	Vertical coordinate above the bed	[m]
z_0	Roughness height in the logarithmic velocity profile	[m]

α	Blockage area by flow	[m^2m^{-2}]
α_d	Plant density as plant area per volume of water	[m^{-1}]
θ	Shields parameter	[-]
τ	Bed shear stress	[Nm^{-2}]
κ	Von Kármán's constant = 0.4	[m]
λ_a	Arc-wavelength of the channel	[m]
λ_m	Meander wave length	[m]
λ_s	Bed disturbance adaption	[m]
λ_w	Flow adaption length	[m]
ρ_s	Specific sediment density	[kgm^{-3}]
ρ_w	Specific water density	[kgm^{-3}]
φ	Angular amplitude	[degree]
φ_0	Maximum angular amplitude	[degree]

1. INTRODUCTION

Insight in the evolution of meandering river systems shifts the attitude of river managers from removing vegetation to reduce flooding to incorporate vegetation as an integral part of the river system. Research has focussed on finding the physical controls by vegetation to explain the wide range of patterns of rivers. The role of vegetation seems very important to balance the formation and destruction of the floodplain (Kleinhans, 2010). In meandering systems very distinct patterns of vegetation patches are created, which align neatly along the channel, see Figure 1-1. These patches induce hydraulic resistance by the obstructing presence of vegetation, which reduce mean flow velocities and increase mean water levels.

Research has focussed on the characterization of flow velocity changes at the stem and leaf scale of relative small vegetation patches in streams and tidal environments, however vegetation resistance at a reach-scale is most relevant to river management (Nepf, 2012). So far, no study examined the hydraulic responses by varying the location and the number of vegetation patches under controlled conditions. This study will support the recent developments to combine biological and fluvial dynamics in modelling studies to further explore the dominant channel and floodplain interaction, which eventually will assist in long-term river design measures.

In order to test effects of vegetation patterns on point bars in meandering river, this study varied the position of typical floodplain vegetation patches with an idealized meandering system in the existing state-of-the-art hydrological model, Delft3D (Lesser et al., 2004). The model is used to quantify the flow distribution for various flow regimes, vegetation types, positions of vegetation patches and number of patches.

This master thesis is connected to REFORM, a European partnership for sharing knowledge and promoting best practices in river restoration. The objective of REFORM is to provide a framework for improving the success of hydrogeomorphological restoration measures to reach, in a cost-effective manner, the target ecological status or potential of rivers ("Buijse, 2014").
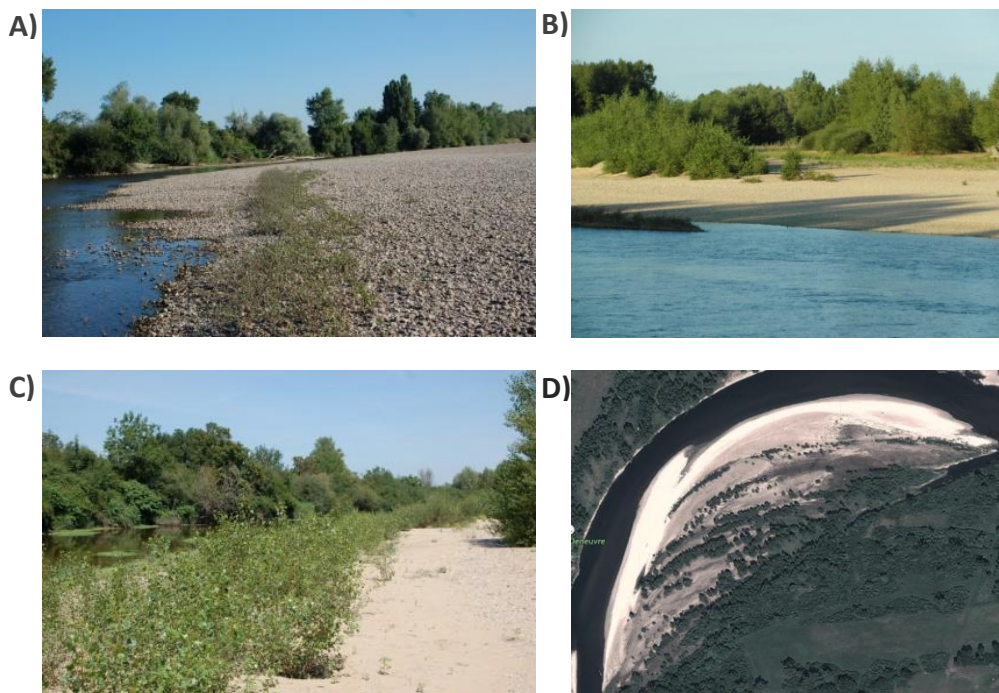
Figure 1-1 Various stages of vegetation patches accurately align along the main channel of the river Allier, France. The patch alignment show ascending development stages higher up the floodplain.

1.1. REVIEW ON VEGETATION PATTERN CREATION IN A MEANDERING SYSTEM

The presented vegetation patterns in Figure 1-1 are a result of the fluvial processes in a meandering system. The control of dynamic meandering over the floodplain and the hydrological connectivity with the floodplain on the development of the vegetation patches are reviewed in this section.

1.1.1. DYNAMIC MEANDERING INTERACTS WITH THE VEGETATION PATTERN

A meandering river is characterized by a single, sinuous channel, which migrates laterally, see Figure 1-2. There is a distinct difference between irregular single channels and meandering channels, namely the meandering river is laterally active and the channels tend to move over the floodplain. Active meandering is a result of a retreating eroded outer bank and an expanding inner bank. There is a balance between the formation and destruction of these banks. The resulting bathymetry in river bends is controlled by a combination of transverse sloped bed by the curvature of the bend and the bar patterns induced by upstream perturbations. Pattern-independent variables can estimate the potential specific stream power to predict the alluvial form (Kleinhans and Van den Berg, 2011). These channel dynamics are relevant for creating the vegetation patterns and the vegetation partly controls the meander morphology.

The planimetric evolution of a meandering river, controlled by continuous elongation, deformation and downstream migration of meanders, and the statigraphic characteristics of the sediments set the conditions for vegetation development. The statigraphic characteristics of river-deposited sediment differ in water-holding capacity, the height of capillary rise, hydraulic conductivity, nutrient levels and water balance throughout the soil column (Merigliano, 2005). Furthermore, the riparian vegetation development depends on the river patterns and the evolution of the river channel. Point bar migration and cutoff events are dominant in the development of the vegetation patterns on the floodplain (Hupp and Osterkamp, 1996; Perucca et al., 2006; Camporeale et al., 2008; Van Dijk, 2012).

As a result of point bar migration, the inner bend becomes a potential vegetation establishment site (Bendix and Hupp, 2000; Perucca et al., 2006). Herbaceous vegetation, such as Salix and Populous seedlings, occupy the point bar, which are aligned with the main channel. The succession stages of vegetation are laterally visible on the point bar, as a result of the settlement patterns of the vegetation. Younger and less developed vegetation are positioned at the channel margin, because the pioneer vegetation establishes at the toe of point bars close to the waterline. Over time, as the channel migrates, the pioneer vegetation develops to fewer, older and more spatial isolated stands (Stella, 2011). The vegetation on higher floodplain is less disturbed by floods and develops to more mature vegetation (Bendix and Hupp, 2000). Figure 1-3 A) shows the schematic development of vegetation patches on a point bar, B) indicates the channel migration of a meandering section of the river Sacramento, where the relation between vegetation stages and the channel migration is visible with the classification of mature vegetation patches in C).
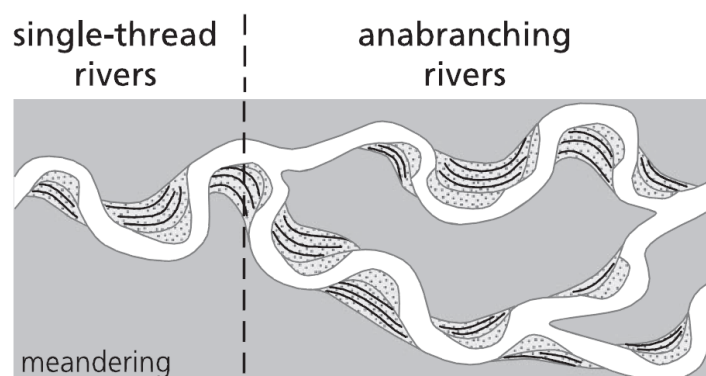
Figure 1-2 A meandering river is laterally active and shows regular sinuous forms, whereas a straight channel shows irregular sinuosity. Such meandering systems can consist of single or multiple channels (Kleinhans and Van den Berg, 2011).
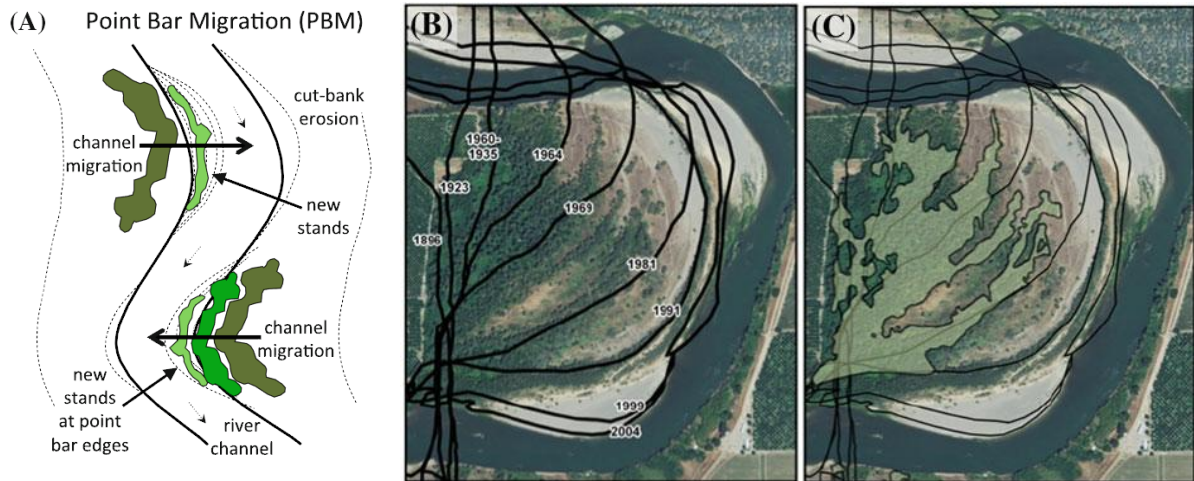
Figure 1-3 Point bar with laterally aligned vegetation patches as a results of meander planform evolution. A) shows the development schematically, B) the historical development and C) the classified riparian vegetation. The alignment to the channel follows the channel pattern (Stella et al., 2011).

Several numerical modelling studies, which incorporate meander evolution and vegetation, also confirm the dominance of morphological changes on vegetation patterns. Perucca et al. (2006, 2007) demonstrate the control of meandering evolution on the vegetation pattern in a model study and advocate for the necessity of coupling the river morphodynamics to the vegetation evolution to explain the visible patterns of vegetation. More recently, Nicholas (2013) developed a general framework for the co-evolution of river and floodplain dynamics. The simulation evolves from a straight channel to a dynamic meandering system with vegetation patches on the inner bend floodplains, which also show the distinctive arc-shaped patterns of vegetative patches and the time patterns of the vegetation as the meander evolves, see Figure 1-4.
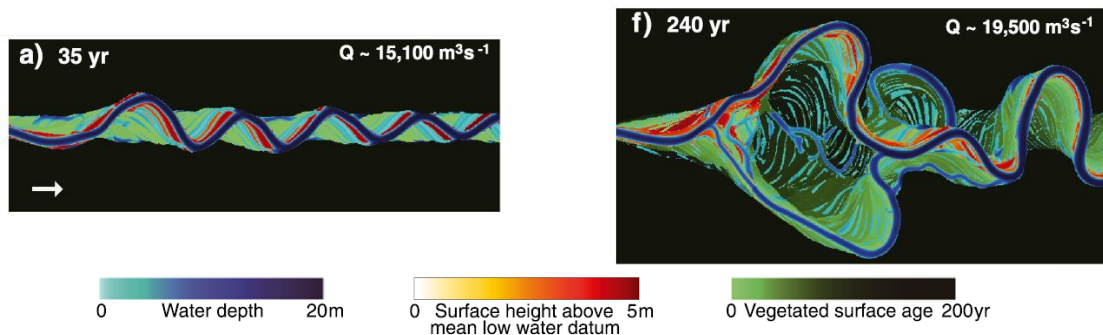
Figure 1-4 The modelled vegetation patches show arc-shaped patterns along the meandering channel, which indicates a gradient of vegetation age along the floodplain. The modelled evolution of this meandering system is over a period of 240 years. Flow is from left to right as indicated by the arrow (Nicholas, 2013).

1.1.2. HYDROLOGICAL CONNECTIVITY INTERACTS WITH THE VEGETATION PATTERN

The hydrological connectivity with the vegetation development in the riparian corridor is strong. Flow influences the vegetation development in two ways, (i) the river provides the recourses for the establishment and growth of vegetation and (ii) the variability of the discharge set back the vegetation development.

First of all, flow processes interact with vegetation through the establishment of vegetation. Seeds distribution by flow on the pointbar is dominant in riparian zones for creating the natural vegetation patterns (Gurnell et al., 2012). Seeds are forced into the inner bend by helical flow (Gurnell et al., 2008). Helical flow is related to the morphology of the meandering channel creates secondary flow patterns (Furguson et al., 2003). The overbank flow distributes the seeds over the floodplain. With the increase in hydraulic resistance of the floodplain, the flow velocity level and the seeds can settle. The main pioneer vegetation species are Cottonwood, Populus or Salix (Van Splunder et al., 1995). The success of establishment of this pioneer vegetation is a combination of root growth and moisture content (Mahoney and Rood, 1998; Camporeale et al., 2008). The river provides the necessary water, nutrients and sediments into the riparian zone. The distribution and growth of the seedlings and the supply of soil moisture influence the vegetation pattern (Camporeale et al., 2008; Gurnell et al., 2012).

Furthermore, vegetation development can be set back by influences of the stochastic variability of discharge. Floods can induce death of vegetation due to burial, uprooting or anoxia (Green, 2005a; Corenblit et al. 2007). Whether a particular high water event will produce the necessary conditions for the establishment of vegetation or physical destruction or uprooting depends on the duration, intensity, frequency, and timing in the year (Hughes, 1997; Vreudgenhil, 2006). In addition, the fluvial disturbances modify plant species composition by eliminating the non-riparian species. Because non-riparian species are intolerant to the physical disturbance regime, whereas the riparian species require these conditions to establish, survive and reproduce (Merritt et al., 2009).

Besides higher water discharges, vegetation has to cope with droughts, which consequently leads to wilting, leaf death and reduction in canopy volume (Gurnell et al., 2012). More extreme droughts result in branch dieback or stand mortality, which results in reducing the leaf area and therefore the hydraulic resistance. This will reduce water stress for surviving branches or individuals (Merritt et al. 2009). The vegetation adapts to water stress and decreased availability of soil moisture. Bendix and Hupp (2000) show this lateral connection schematically, with an ideal location for establishment of vegetation, see Figure 1-5.
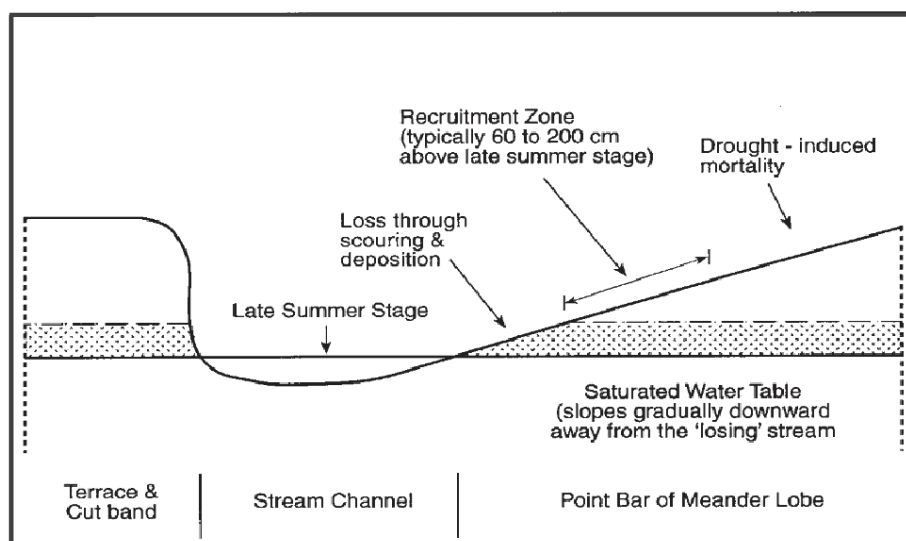
Figure 1-5 Cross-section of potential establishment sites for vegetation patches, where success is large determined by floodplain height (Bendix and Hupp, 2000).

1.2. REVIEW ON HYDROLOGIC RESISTANCE INDUCED BY VEGETATION PATCHES

This study is focuses on the described patterns that are caused by the hydrological connectivity and the morphological changes in the meandering corridor. The hydraulic resistance induced by vegetation stands, the description of this hydraulic resistance and the hydraulic response is reviewed in this section.

1.2.1. HYDRAULIC RESISTANCE

The presence of vegetation in the flow field causes a local increase of the hydraulic resistance (e.g. Järvelä, 2004; Corenblit et al., 2007; Nepf, 2012). The flow needs to go through, around and over the vegetation, which creates drag along the vegetation stems, turbulence and diffusion within the vegetated region and the wake behind the vegetation. Consequently it generates flow retardance and the water sets up at the leading edge of the vegetation patch. Several factors of the dimensions of the vegetation determine to which extent and how the flow is modulated, based empirical studies.

Vegetation induces skin and form drag, which explains the flow resistance. Flow roughness is the energy dissipation caused by the resistance of the surface, here referred to as skin drag. The skin drag describes the bumpiness of the flow surface. Secondly, form drag is the result of the channel geometry. There are vortices formed in the flow, which initiate energy losses. Objects that obstruct the flow occur as form drag, e.g. vegetation structures or bed forms. The flow that moves through the porous vegetation patch is altered by the vegetation patch. The flow recirculates directly behind the patch, see Figure 1-6. There is also a wake created downstream of the vegetation, which actually lowers the water depth, besides reducing the turbulence and flow velocities (Nepf, 2012).

The effect of form drag is commonly expressed by empirical methods using scaling assumptions (Huthoff, 2007). The drag, which is induced by the presence of an object, results in a pressure drop in the wake of the object. The area of a pressure drop increases for a larger wake. This wake region is closely related to the blockage area of the vegetation (Nepf, 1999). The drag force (F_D) on an object within a flow field is determined by the following:

$$C_D = \frac{F_D}{\frac{1}{2}\rho_w \alpha_d U^2}$$

Equation 1-1

where C_D is the drag coefficient, ρ_w is the water density, U is the equivalent uniform velocity and α_d is the blockage area by the vegetation in the volumetric channel.
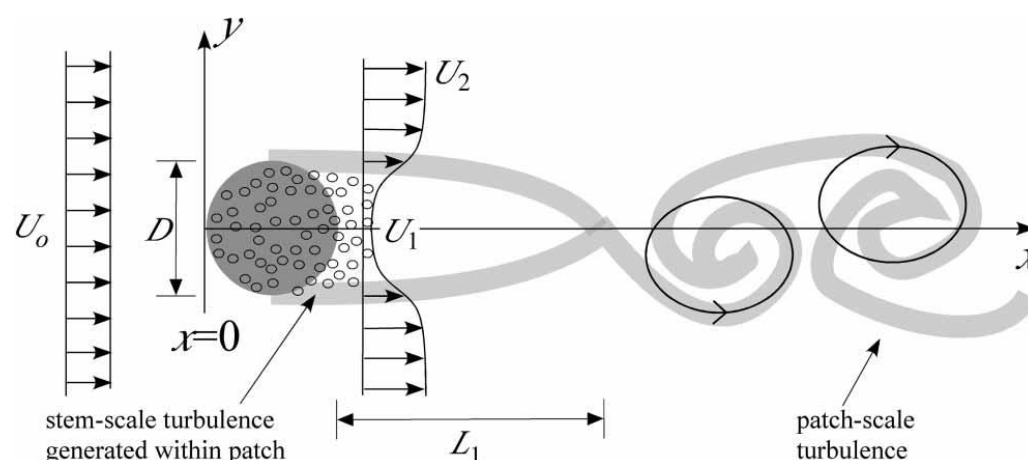
Figure 1-6 Top-view of a round vegetation patch inducing stem-scale and patch-scale turbulence. The stem-scale turbulence is slowing down the flow within and close to the vegetation patch. The wake behind the vegetation patch forms a vortex street, which has a larger downstream extent (Nepf, 2012).
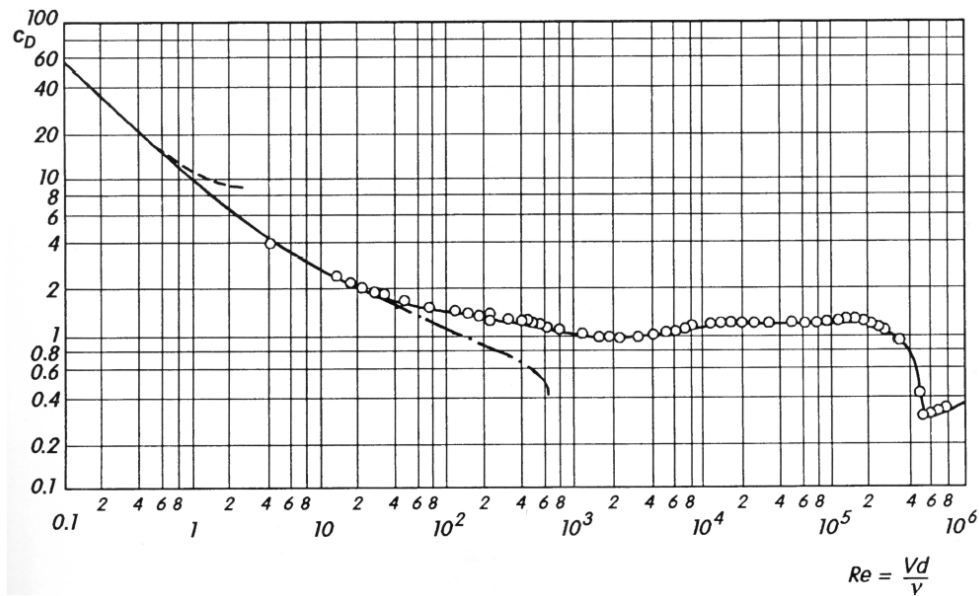
Figure 1-7 The blockage describes the drag by an obstructing object well. As a result of a constant drag coefficient, $C_D \approx 1$, with turbulent flow (Re $10^2 – 10^5$) (Schlichting and Gersten, 2000).

The empirical drag coefficient is related to flow around rigid cylinders for varying turbulent flow in Figure 1-7. In laminar flow conditions (Re<2000) C_D is inversely proportional to the Reynolds number (Re). For more turbulent flows, the drag coefficient is approximately 1. This suggests that the blockage area of an object is a sufficient indicator for describing the drag (Huthoff, 2007). However, for high turbulent flow (Re > 10^5) this relation does not hold. Section 1.2.2 will further elaborate on the physical characteristics and the quantification of the hydraulic resistance specifically for vegetation.

1.2.2. DESCRIPTION HYDRAULIC RESISTANCE

Several studies attempt to describe the hydraulic resistance in a general and applicable way for river studies with vegetation. Hydraulic resistance of homogenous vegetation in a straight flume depends on many variables, such as stem density, water depth, flexibility, incoming flow velocity at the leading edge (Järvelä, 2002; Nepf, 1999). Authors emphasize on a horizontal blockage area as a single descriptor to explain the presence of vegetation within the volume of water Green 2005b; Baptist et al., 2007; Nikora et al. 2008 and Nepf and Vivoni, 2012), although the planview area also correlates surprisingly well, which is easy to determine in the field or even from images above (Green, 2005a).

To quantify this obstruction of vegetation, this study focuses on the description developed by Klopstra (1997) and Baptist et al. (2007). The description uses physical-based resistance descriptors for the logarithmic velocity profile, which is therefore also applicable for submerged vegetation. Baptist et al. (2007) divides the velocity profile over vegetation into four zones: 1) near the bed 2) just below the top of the plants 3) the top of the plant 4) above the vegetation. This is schematized in Figure 1-8. The two most important zones, according to Baptist et al. (2007), are the zone inside the vegetation, zone 1), the velocity is in this zone is constant. The second zone is the zone above the vegetation, zone 4).
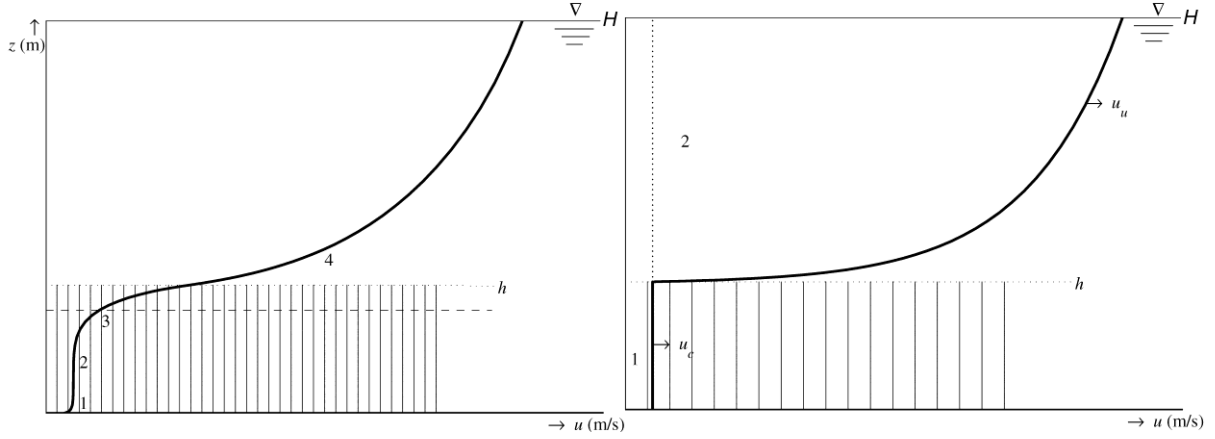
Figure 1-8 Typical schematized velocity profiles for vegetation in the water. A) Vertical profile of horizontal flow velocity for submerged vegetation with four flow regimes. B) The predicted flow velocity profile, based on Equation 1-2 and Equation 1-3 (Modified from Baptist et al. (2007)).

The flow velocity inside the vegetation, zone 1, assumed to have a uniform profile, which is also confirmed by others (Zong and Nepf, 2010). See Figure 1-8 for the definitions of the zone to the velocity profiles. The vegetation height (h) and the density of the vegetation (m), which is given by the number of stems per square meter (n_s) and the diameter of a single stem (d), determine the velocity inside the (submerged) vegetation (u_c).

$$u_c = \sqrt{\frac{Hi}{\frac{1}{C_b^2} + \frac{C_D n_s dh}{2g}}}$$

Equation 1-2

The velocity inside the (submerged) vegetation is also dependent on variables related to the hydrodynamic state of the river itself, such as the water depth (H), the slope of the channel (i) and the reach-averaged Chézy coefficient representing the bed resistance. The logarithmic velocity profile, u_u above the vegetation in zone 2 in Figure 1-8B) adds u_c as a constant slip velocity to match the velocity profiles at the height of the vegetation. The velocity above the vegetation at water depth (z) is given by:

$$u_u(z) = u_* \ln\left(\frac{z-h}{z_0}\right) + u_c$$

Equation 1-3

The extra velocity above the vegetation patch at vertical height above the bed is the natural logarithm of the ratio between this water level above the vegetation and the roughness height for a logarithmic velocity profile (z_0), which was introduced by Nikuradse (1930). Based on these velocity descriptions for the presence of vegetation in the water flow, an equation is found to determine a representative Chézy coefficient. The physical characteristics of vegetation to determine the representative Chézy coefficient (C_r) are the drag coefficient (C_D), which is dependent on the Reynolds number as presented above, the vegetation height (h) and the density of vegetation (product of d and n_s), see Equation 1-4. These spatial characteristics are strongly related to the type and stage of the vegetation. The coefficient is described as a logarithmic profile, see Equation 1-4:

$$C_r = \sqrt{\frac{1}{\frac{1}{C_b^2} + \frac{C_D n_s dh}{2g}}} + \frac{\sqrt{g}}{\kappa} \ln\left(\frac{H}{h}\right)$$

Equation 1-4

1.2.3. HYDRAULIC RESPONSE BY THE PRESENCE OF A VEGETATION PATCH

According to Luhar and Nepf (2013), patch-scale geometry is more relevant than the leaf-scale geometry of the vegetation to modify flow patterns and flow distributions. The presence of vegetation in open-channel flow leads to velocity reduction within the patch and an increase in water depth. Fully developed flow structures within the patch are extensively studied experimentally (Nepf and Vivoni, 2012; Järvelä, 2004) and numerically (Choi and Kang, 2004; Baptist, 2007). As flow enters the vegetation patch at the leading edge and exits at the trailing edge downstream, it needs a transition length to reach a new equilibrium (Ghisalberti and Nepf, 2009) and flow gradients with heterogeneities may be predominant in patches in natural rivers (Sukhodolova and Sukhodolova, 2010; Sinischalchi et al., 2012). The study of Sinischalchi et al. (2012) shows the largest increase in water depth at the leading and a depression at the trailing edge under various hydrological conditions as a result of the presence of a vegetation patch. The water level rise upstream increases as the flow rate increases (high) and reaches to a maximum of 7% relatively to the incoming water depth, which is shown in a longitudinal profile of Figure 1-9. Correspondingly, longitudinal velocity gradients vary within the patch. Velocity inside the patch is strongly reduced and at the trailing edge the velocity has a tendency to return to the undisturbed upstream flow condition (Sinischalchi et al., 2012).

Longitudinal profiles generally show a decrease in flow velocities, whereas transverse profiles also incorporate the velocity changes at the edges of the patch and between patches. These profiles dominantly show an increase of velocity at the edge, because the increased resistance of the patch forces water to flow around the patch (Bouma et al., 2007). Therefore, the presence of vegetation could result more erosion, relative to no vegetation, which limits the development of the vegetation patch (Temmermans et al., 2007). Nepf (2012) also recognizes the importance of the positive and negative feedbacks at the edge of the vegetation patches, which may locally produce enhanced flow structures for lateral expansion of sedimentation and patch development.

The flow can be even further channeled, as multiple patches redirect and therefore accelerate the flow velocity at their edges. Experiments by Vandenbruwaene et al. (2013) present the thresholds for the flow interaction between multiple patches. As the interdistance between the patches relatively to the width of the patch decreases, the patches start to behave as one patch. Figure 1-10 shows the increase of velocity at the edge of the patch for various diameters of the patch on the left side of the graph. The right side of the graph shows the concentrated flow by the multiple patches for various diameters and distances between the patches. The positive relation between the flow acceleration and the patch size suggests that channel formation is more likely around larger patches (Vandenbruwaene et al., 2011).
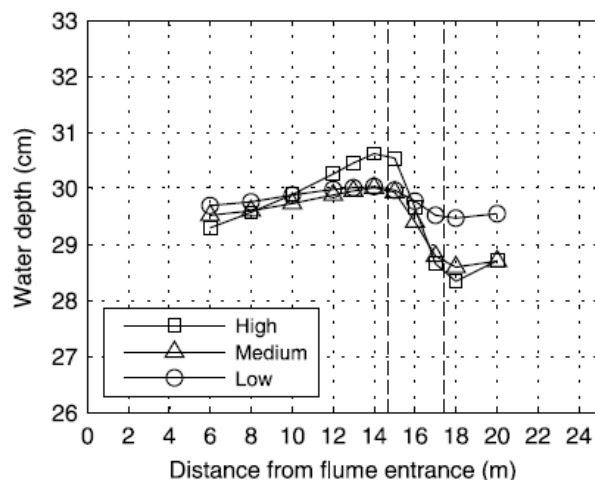
Figure 1-9 Water depth increases at the leading edge and decreases at the trailing edge of the patch. The dashed lines define the vegetated edges of the patch (Sinischalchi et al., 2012).
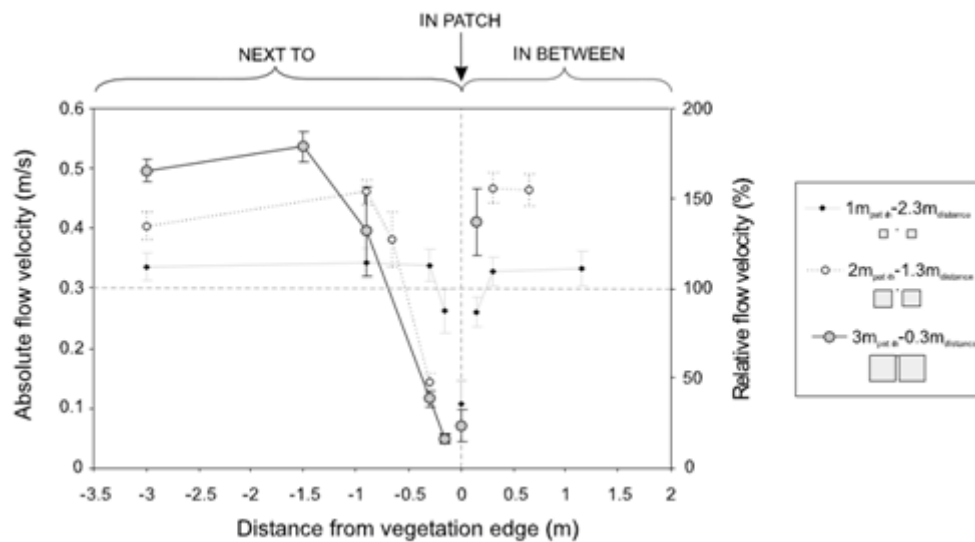
Figure 1-10 Transverse profiles show an increase in flow velocity at the along edge and between patches. Where the edge is shown with a negative distance and the absolute flow velocity between two patches is related to a positive distance from the patch (Vandenbruwaene et al., 2013).

1.3. GAPS IN KNOWLEDGE

Interactions between vegetation and fluvial processes are widely recognized and addressed. Individual descriptions of flow through and over vegetation are studied extensively, as well as the cumulative water level rise of vegetated floodplains with much heterogeneity in the vegetation. Furthermore, the creation of the specific patch alignment and their variation within meandering river systems is known. However, the combination of the water set up in front of vegetation patches and the variation in the velocity field as a result of various locations of the vegetation patches is yet not identified in a river system. These variations in the hydrodynamic response could be relevant for river and floodplain manager to assess the flood security and manage embankments and floodplains of rivers, as more room for natural processes in the river corridor is promoted. Also the patch location redirects flow patterns in the river system, resulting in an increased floodplain or channel flow.

In order to analyse the water set up in front of the vegetation patch and changes of the velocity field as a result of the presence of the vegetation patches, a systematic analysis of various locations of the patch(es) is needed at a single meander wavelength scale. Sophisticated modelling software offers the opportunity to study these effects at a larger river reach scale for different vegetated banks as extensive experimental work on the hydraulic resistance can support the study of these patterns can numerically be studied.

1.4. HYPOTHESES

Three hypotheses are extracted from the review on vegetation patterns and its hydrodynamic response. The questions in the section hereafter are based on these hypotheses.

- *As vegetation obstructs the flow, water rises in front of the patch at the leading edge and redirects flow around the vegetation patch with lower flow velocities within and higher velocities at the edges.*

- *Multiple vegetation patches will act as one vegetation patch with a relative small distance between the patches to the patch width, which results in a higher water level rise and stronger flow redirection.*

- *Vegetation patches on the floodplain will redirect the flow through the channel, with a stronger redirection as more blockage by vegetation is induced on the flow.*

1.5. RESEARCH QUESTIONS

This study focuses on the importance of variations in location of vegetative patches. Distinctive vegetation patch alignments are created along the meandering river. This thesis aims to find the variation in hydrodynamic response by changing the locations of the vegetative patches along the meander reach.

As the meandering system evolves, the relative distance of the vegetation patch to the channel is larger. Consecutive arc-shaped patches are the result. These variations in position of the vegetation modulate the hydraulic response, e.g. higher water levels in front of the vegetation and flow diversion over the floodplain and main channel. To get more insight in these physical effects on a near field (5 water depths around the vegetation) and a far field scale (single meander bend and whole reach) the following questions arise:

- *How does variation in the position of vegetation patches effect the raise in the water level within and near the vegetation patch?*

- *How does variation in the position of vegetation patch redirect the velocity patterns within and near the vegetation patch?*

Scroll bars are formed as the meander bends migrate, which seem to be favourable locations for riparian vegetation to settle and as time accumulates, multiple vegetation patches occupy the floodplain. The evolving meandering system, without cut-off events, increases the number of vegetative patches on the floodplain. Therefore the following two sub questions are defined:

- *How does variation in the numbers of vegetation patches raise the water level within and near the patches?*

- *How does variation in the vegetation patch number redirect the velocity patterns within and near the vegetation patch?*

The blockage by the vegetation can create two preferable flow paths, namely the shortest over the higher floodplain or through the main channel with a higher flow velocity. Furthermore, blockage changes as the position on the floodplain is varied for different types of vegetation as well as the number of patches. Systematically approaching this variation will lead to insight in the hydraulic response of giving room to natural processes on the floodplain. The following question arises:

- How does the blockage by various positions and the number of vegetation patches control the redistribution of discharge over the floodplain?

1.6. STRUCTURE OF THIS THESIS

First, the developed method is described that is used to execute the simulations and evaluate the hydrodynamic effects in (Chapter 2). Hereafter, the results and the interpretation for the near field and far field hydrodynamic responses are presented for changing distances and number of patches (Chapter 3). The reliability of the results is discussed and compared to findings of other studies (Chapter 4), followed by the answers to the research questions (Chapter 5). The complete overview of all results of the simulations is shown in Appendix I, II, III and IV. Supplementary data and codes can be obtained by contacting the author and the data structure is presented in Appendix V.

2. METHOD

In this chapter, the developed methods to create and analyse the position variation of vegetation patches in a meandering river are described. First, the morphology based on bar theory and the Kinoshita-generated curve is described to use as a static morphology in the Delft3D modelling software. Thereafter, the method to change height, the position and number of patches on the pointbar is explained. Thirdly, an overview of the conducted simulations in this study is provided. In the last section describes the evaluation of the hydraulic response by the vegetation patches.

2.1. MORPHOLOGICAL BOUNDARY CONDITIONS

The morphodynamic domain represents an idealized version of the geometry that is commonly observed in meandering systems. In order to avoid hydrodynamic responses by variation in morphology and increase the reproducibility of this method, an idealized meander structure is developed. The following section is primarily the design stage of an asymmetric meandering channel planform, which covers the estimation of the theoretical prediction of the meander length based on bar theory and the description of the centreline of the meandering system with the related cross-section.

2.1.1. BAR THEORY

The prediction of the meander wavelength of a meandering system is based on bar theory, which assumes an upstream perturbation. The meander wavelength dimensions can be predicted by the equations of Struiksma et al. (1985), which predicts the forced bars. This theory is further explored by Corsato and Mosselman (2009) for multiple bars and they developed an interaction parameter (IP). The meander topography can be understood as the interaction between the transverse bed, related to the local channel curvature and a sequence of steady bars induced by channel curvature perturbations upstream (Kleinhans and van den Berg, 2011). First the characteristic adaptation length of flow (λ_w) is estimated, based on the Chézy's coefficient (C), which is given in Equation 2-1.

$$C = \frac{\bar{u}}{\sqrt{\bar{H} * i}}$$

Equation 2-1

where i represent the channel slope and $\bar{H}$ the reach-averaged water depth and λ_w can be estimated as in Equation 2-2.

$$\lambda_w = \frac{C^2 * \bar{H}}{2g}$$

Equation 2-2

The adaption length of a bed disturbance in the cross-sectional river bed profile (λ_s) is dependent on the transverse bed slope effect (f(θ)).

$$\lambda_s = \frac{\bar{H}}{\pi^2} * \left(\frac{W}{\bar{H}}\right)^2 f(\theta)$$

Equation 2-3

where W represents the width of the channel. The magnitude of the transverse bed slope effect is calculated as (Talmon et al., 1995):

$$f(\theta) = 9\left(\frac{D_{50}}{\bar{H}}\right)^{0.3} * \sqrt{\theta}$$

Equation 2-4

where D_{50} is the median grain size diameter and represents the sediment in the meander reach and θ is the non-dimensional Shields parameter and is used to determine the initialization of motion of sediment and is expressed as a balance between the bed shear stress (τ) and gravity:

$$\theta = \frac{\tau}{(\rho_s - \rho_w) * g * D_{50}}$$

Equation 2-5

Finally, the non-dimensional interaction parameter is given by:

$$IP = \lambda_s / \lambda_w$$

Equation 2-6

The interaction parameter can be used to calculate the wavelength of the bars, which can be used in order to determine the meander length of a river reach (Kleinhans and Van den Berg, 2011).

$$\lambda_m = \frac{2\pi\lambda_w}{\frac{1}{2}\sqrt{(b+1) * IP^{-1} - IP^{-2} - \frac{b-3^2}{2}}}$$

Equation 2-7

where b is the degree of non-linearity of the sediment transport used for depth-averaged velocity ($q_b = f(u^b)$), which between 3 and 10. The ideal theoretical meander wavelength for a river with conditions similar to the Allier River is 1130 meter, shown in Table 2-1.The description of the evolutionary state of the meander is described in the next section.

2.1.2. CENTRELINE DESCRIPTION

The Kinoshita-generated curve describes the centreline with the predicted meander wavelength. Several formulations for a river planform have been developed, symmetrical bends, such as sine-generated curves (Langbein and Leopold, 1966) and asymmetrical bends, such as Fourier series-based (Yamaoka and Hasegawa, 1984) or Kinoshita-generated (Kinoshita, 1961; Parker and Andrews, 1986; Abad and Garcia, 2009). This study uses the curve described by Kinoshita (1961), as it can describe meandering systems (Abad and Garcia, 2009). The asymmetrical Kinoshita-generated curve is described by an intrinsic streamwise coordinate (s):

$$\varphi = \varphi_0 \sin\left(\frac{2\pi s}{\lambda_m}\right) + \varphi_0^3\left(J_s \cos\left(3\frac{2\pi s}{\lambda_m}\right) - J_f \sin\ s\left(3\frac{2\pi s}{\lambda_m}\right)\right)$$

Equation 2-8

where φ and the φ_0 are the angular and maximum angular amplitude and J_s and J_f are the skewness and flatness coefficient, which represent the asymmetrical behaviour of meanders. The dimensions characteristics are based on a fluvial lowland river, the river Allier. The characteristics are shown in Table 2-1. The maximum angular amplitude is set at 60°, which results a state of the fluvial evolution of the meandering system and it is based on the sinuosity (= 1.4) of the meander reach. Lower angular amplitude would represent a less developed outer bend and lower amplitude meanders.

The theoretical river bathymetry and floodplain are presented in Figure 2-1. The simulations of the effects of vegetation patches on the hydrodynamics in the meander reach are situated in this morphology domain. The morphological conditions resulted in a meander wave length of approximately 1130m, which is based on the bar theory discussed in section 2.1.1. Seven meander wave lengths are designed in order to avoid upstream and downstream flow interaction in respect to the third meander bend. The floodplain dimensions are based on the fluvial corridor of the river Allier. The elevation of the idealized floodplain is linearized with the distance to the channel and distance to the floodplain border. A five by five square moving average is used to avoid too high width-depth ratios.

Table 2-1 The parameters and variables, which are used to create the idealized bathymetry. The parameters of the idealized bathymetery are based on the physical representative meandering river Allier, France.

Parameter	Value	Unit	Description
b	5	-	Degree of non-linearity of sediment transport
D_{50}	0.05	m	Median grain size
H_{ch}	1.5	m	Channel depth
H_{fl}	1.85	m	Floodplain height
i	$6.7*10^{-4}$	m m^{-1}	Valley slope
J_f	1/192	-	Flatness
J_s	0	-	Skewness
n_m	7	-	Number of meander waves
S	1.387	-	Sinuosity
$\bar{u}$	1.2	m s^{-1}	Mean velocity in the channel
W_{ch}	120	m	Channel width
W_{fl}	350	m	Mean floodplain width
θ_0	60	°	Maximal angular amplitude related to sinuosity
λ_m	1130	m	Meander wave length
λ_s	243	m	Reach-averaged adaption length sediment
λ_w	114	m	Reach-averaged adaption length water
ρ_s	1000	kg m^{-3}	Specific density of sediment
ρ_w	2650	kg m^{-3}	Specific density of water

The predefined planform and bed formulation presents some limitations, such as the assumption of a river bed in a steady state condition with no point bar migration and outer bank erosion. First of all, the meandering dimensions, e.g. meander wavelength, are based on bar theory. Bar theory requires the actual channel width and channel gradient downstream. The measured width and channel gradient are strongly pattern-dependent (Kleinhans and Van den Berg, 2011). Predictions of pattern-independent widths and gradients generally over estimate the widths of meandering channels, such as in the study of Parker et al. (2007). More sophisticated predictions include bank strength (Eaton and Church, 2007). However, it would require information on the floodplain composition of the sediments and vegetation. This is outside the data availability and therefore outside the scope of this study. Secondly, the Kinoshita-generated curve describes the thalweg of the meandering channel and represents a certain development stage of the meandering channel (Abad and Garcia, 2009). The maximum angular amplitude varies for different stages of a meander bend. This amplitude for this study is based on the average sinuosity of the Allier and kept constant for all meanders in the reach. The heterogeneity of meander bends in a meandering reach is not covered in this study, although the overbank flow differs for various meander amplitudes.

Even though this methodology represents an idealized meandering bathymetry, it can support studies with a constant or an initial bathymetry in a dynamical equilibrium to study flow patterns for river restoration, placement of structures in meandering systems and vegetation development. Modelling outer bank retreat and bank accretion is still under development within Delft3D (Spuyt et al., 2011) and since the computations will take a large amount of time to come to an equilibrium profile, a constant and idealized bathymetry is useful to study the hydrodynamic response by the presence of vegetation structures on the floodplain. Furthermore, analysis can be done on a river reach scale as vegetation is placed on a reparative morphology throughout the reach, which isolates the hydrodynamic response of the vegetation patches.
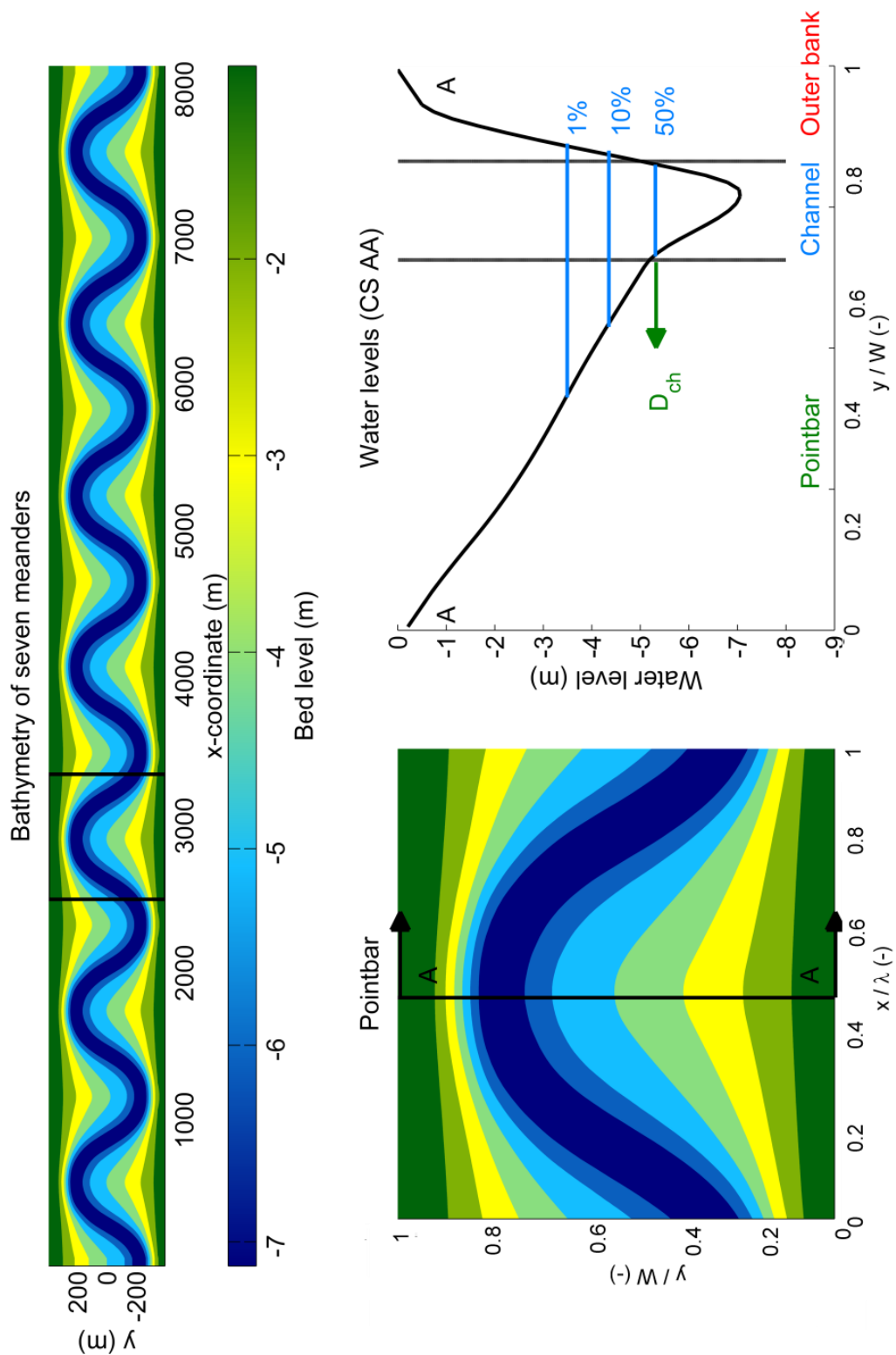
Figure 2-1 Overview of the morphodynamic meandering system used in the simulations. The meander length of the Kinoshita-generated curve, which represents the thalweg, is based on bar-theory and results in the idealized meandering system. A) The plan view of an idealized bathymetry, where the floodplain height is an interpolation between the distance to the main channel and floodplain boundary. B) Plan view of the third single meander, which is used to study the near-field hydrodynamic responses. The height definition of the channel and the floodplain are visible by the steep slope of the outer bank and a low height gradient of the point bar. C) The cross-section of A-A with the water levels for three flood events with an occurrence of 1%, 10% and 50%, where the median water level defines the distinction between the channel and the floodplain.

2.2. HYDROLOGICAL BOUNDARY CONDITIONS AND THE CONTROL SIMULATION

The simulations are carried out for a medium and high flood event in the meandering system. Observations of the discharge at the river Allier are the basis for these hydrological conditions. During the simulations, there is no variation of the discharge. The medium and high hydrological conditions have a discharge of respectively 250 and 500 m^3/s. These have an occurrence per year of respectively 10% and 1%. Figure 2-2 shows the frequency for the different water depths corresponding to the different discharges, where the blue lines indicate the flood events used in this study. The discharge leads to static state water level, as a result of no change in the hydrodynamic and morphological boundary conditions. The water levels for the meandering system relative to the bed level are shown in Figure 2-1C. These water level differences correspond with measurements, shown in Figure 2-2B.

The water depth, flow velocities, Froude number and Shields number of the control simulation, the simulation without vegetation, for high discharge are visualized in Figure 2-3 for two meander wavelengths. The vegetation is placed in this hydrodynamic regime. The maximum water depth in the main channel during a high flood event is 3.2m and maximum flow velocities are approximately 1.1 m/s. The combination of water depth and velocity result in the Froude number, which shows the flow is most critical upstream of the apex, but remains subcritical throughout the reach (<1). The Shields number represents the mobility of sediment of the river Allier in water flow and is a non-dimensionalization of the shear stress, see Equation 2-5. The water level and velocities shown in Figure 2-3 are used as a reference to compare the results of the simulations with vegetation patches.
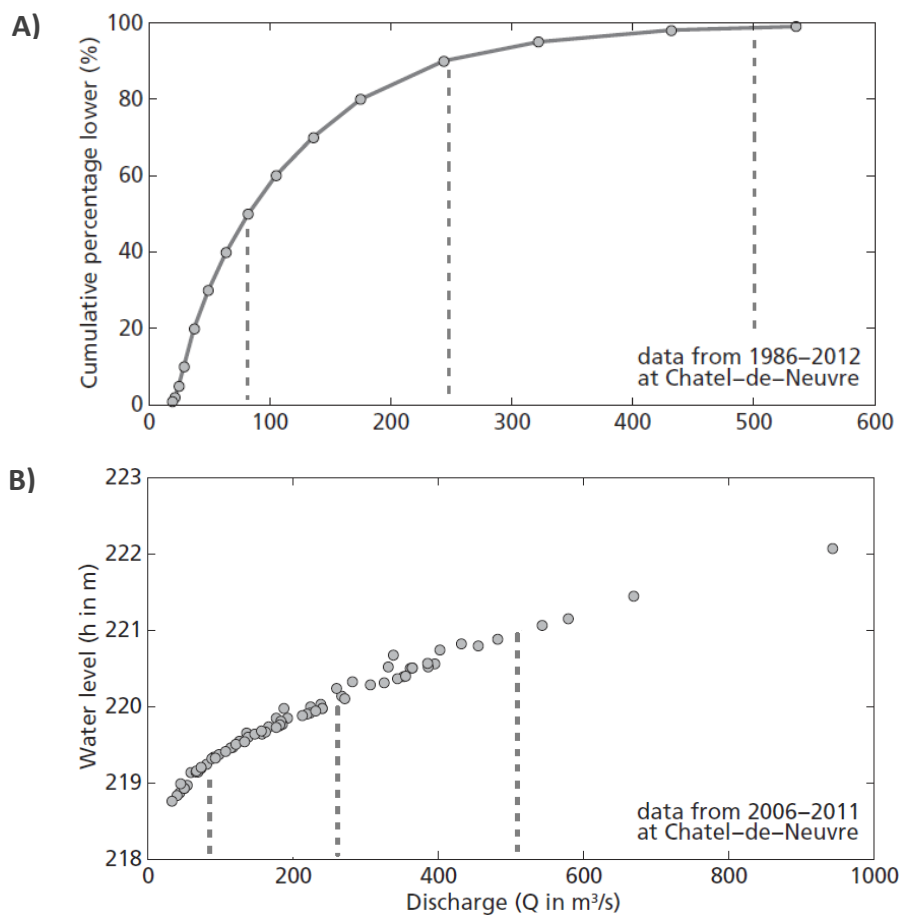
Figure 2-2 Characterization of the hydrology of the river Allier for 1986-2012. A) Discharge of the river Allier for a station at Châtel-de-Neuvre and B) Observed water levels in relation to the discharge of the river Allier (Modified from Van Dijk (2013)).
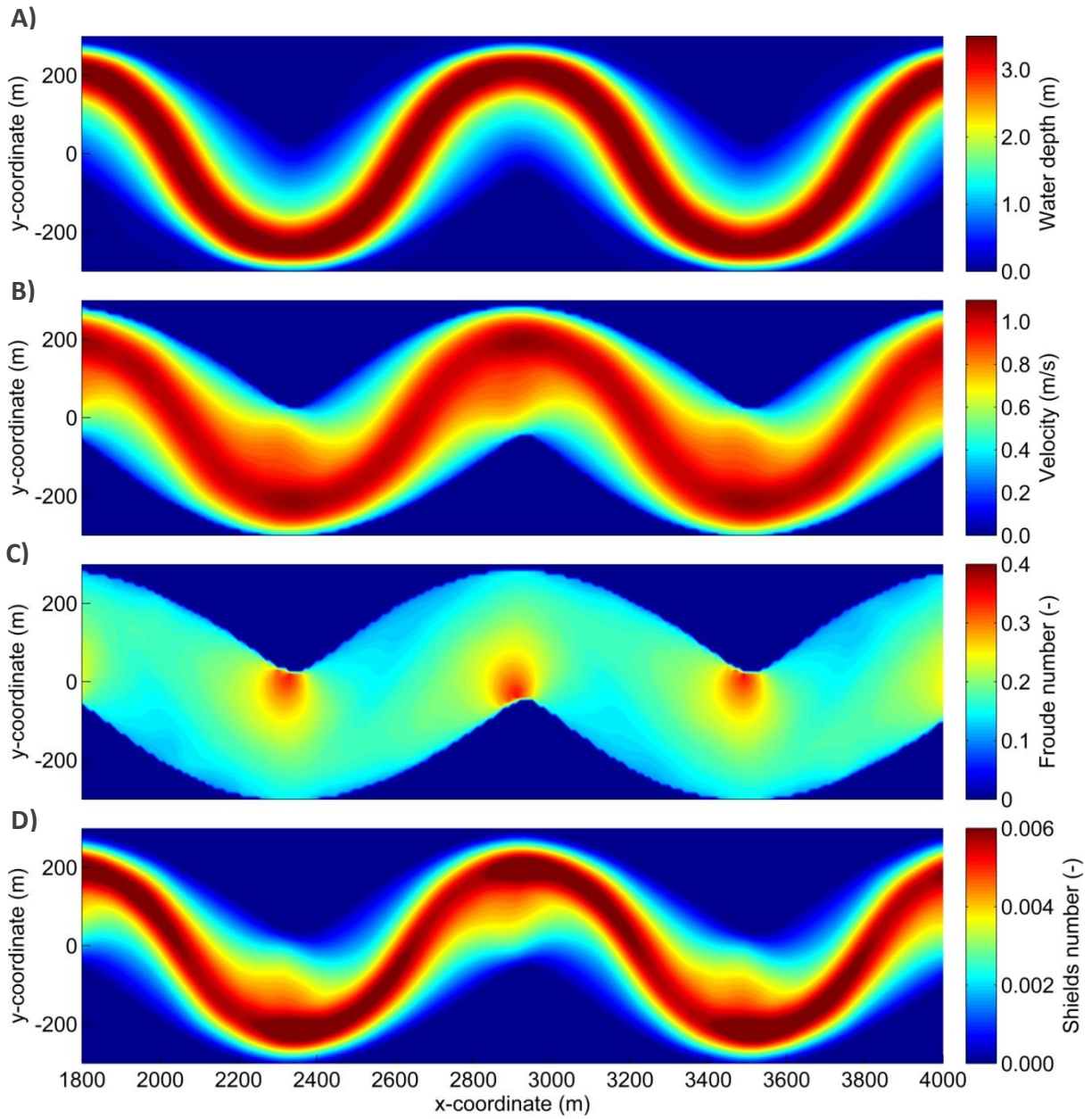
Figure 2-3 The hydrodynamic regime for the control simulation for two wavelengths with high discharge (Q = 500 m^{3}s^{-1}). A) Water depth, B) depth-averaged velocity, C) Froude number and D) Shields number with D = 5.0 mm.

2.3. VEGETATION REGIME

The hydro- and morphodynamic conditions are used as the boundary conditions to incorporate the vegetation on the floodplain. First the structural characteristics of the vegetation are described. Secondly, a suitable description of the position of a single patch on the floodplain is presented. The simulations incorporate the evolving river and the related change of position of the patch relative to channel, which is summarized in section 2.3.3.

2.3.1. INDIVIDUAL VEGETATION DESCRIPTION

Baptist et al. (2007) describes the physical characteristics of vegetation within the Delft3D model. His quantification of the hydraulic resistance is applied in this study. Several types of riparian vegetation are present on the floodplains of the river Allier. This study focuses on the position of the vegetation and the development stage is strongly related to the position of the vegetation on the floodplain (Bendix and Hupp, 2000). Therefore two representative vegetation types, herbaceous vegetation (small) and softwood shrub (large) are placed in the meander reach. These vegetation types are common on the floodplain of the Allier (Geerling et al., 2006) and have a sufficient hydrodynamic impact to study the effects of various patch positions. The vegetation patches in this study have a uniform height, stem density and diameter, based on empirical data by Van Velzen et al. (2003). These vegetation characteristics are all attributes at the canopy scale, which are measureable geometrical properties of vegetation in the field. However, the drag coefficient is not directly measurable and is generally used as a calibration parameter. The drag coefficient can be considered to account for the complex structure of vegetation, such as foliage and the vegetation roughness, discussed earlier. The physical parameters inducing the hydraulic resistance of the vegetation are given in Table 2-2.

The homogenous vegetation patch is a strong simplification of the real world complexity of vegetation structures within a patch. Nevertheless this simplification is suitable for this study to simulate and compare the hydrodynamic response of the variation of the location of the patch and the number of patches. Therefore the height, density and type of vegetation are homogeneous throughout the patch and the simulations can be executed in a controlled environment.

2.3.2. VEGETATION PATCH SHAPE AND POSITION

The location of the riparian vegetation can be verified by the days of inundation per year for this specific river system, as the hydrological connectivity with the floodplain dominates the positioning of the riparian vegetation. In order to get a global identification of the position of vegetation, Duel and Specken (1994) developed a habitat suitability index (HSI) for willow and poplars, which incorporates the inundation duration per year. The vegetation needs enough water to prevent drought-induced vegetation decline or even mortality, however too many days of inundation per year discourages the settlement of riparian vegetation. Table 2-3 defines the habitat suitability index for the different inundation periods per year. With the discharge distribution of 1%, 10% and 50%, an indication of the HSI is determined for this meandering system.

Table 2-2 Overview of the vegetation characteristics of herbaceous and softwood shrub. These characteristics are used to determine the velocity profile and results in a representative Chézy coefficient and correspond to typical riparian vegetation in the river Allier, France (Van Velzen, 2003).

Parameter	Description	Unit	Small	Large
H	Vegetation height	m	0.56	6
n_v	Vegetation density	-	0.23	0.13
C_D	Vegetation drag coefficient	-	1.8	1.5
w	Width of the vegetation patch	m	20	20

Table 2-3 Habitat suitability index for riparian vegetation, which is based on the inundation time per year (Duel and Specken, 1994).

Inundation time (days/year)	HSI
< 50	0
50 - 65	0.3
65 - 80	0.7
80 - 140	1
140 - 165	0.7
165 - 180	0.3
> 180	0

The resulting HSI for the control simulation show good agreement with natural arc-shaped vegetation patches presented in Figure 2-4, which presents all non-zero elements. The bathymetry is used as a background, where the HSI is zero. Further analysis will provide results on the self-reinforcing character of vegetation and whether the inundation time is a representative indicator for the settlement of vegetation.

The position of the patch in the simulations is between the two inflection points of the meander with an initial distance of 50 meters to the water line and the width of the patch is 20 meters. The variation in patch position over the floodplain will not change the dimensions of the patch and the patch will only be shifted relative to the channel over the apex. For simulations with multiple patches, the exact same positions are used at 100, 150 and 200 meters from the channel.
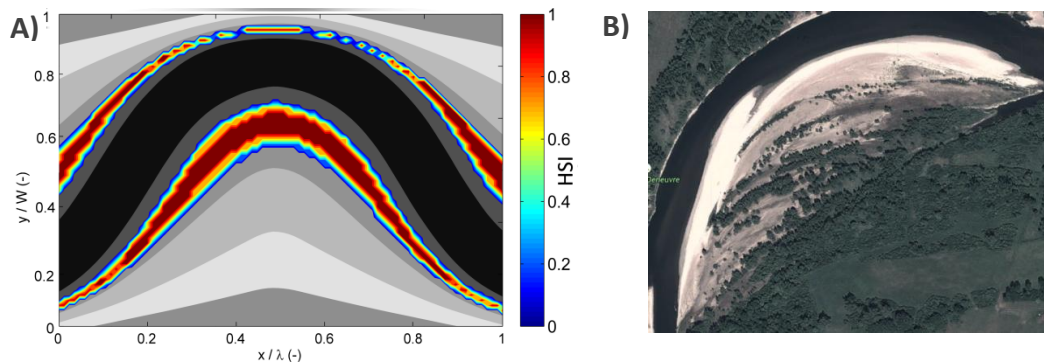
Figure 2-4 The habitat suitability index and the natural patterns correspond visually. A) HSI for riparian vegetation for the third meander in the meandering planform. The HSI indicates favourable positioning of the vegetation along the fluvial corridor and is arc-shaped. B) Vegetation on the floodplain of the river Allier, where the vegetation pattern corresponds to the vegetation position indicated by the HSI.

2.3.3. SUMMARY OF SIMULATIONS

The variation of the vegetation position can be considered as meander migration. The distance of the vegetation relative to the channel increases, as the meandering channel evolves to a higher asymmetry. In order to study this floodplain process, simulations with Delft3D are carried out. Furthermore, the bathymetry will not change, in order to compare the effects of hydraulic resistance initiated by the vegetation are isolated. Therefore, the vegetation is relocated at a greater distance to the channel, D_{ch}. The relocation of the vegetation patches is studied under different hydrodynamic regimes, namely 1% and 10% reoccurrence flood events.

Table 2-4 Overview of the simulations to determine the hydrodynamic response by various positions and number of patches, under various hydrological conditions for different riparian vegetation types.

Q	Q = 250 m³/s Veg = small D_{ch} = 100 m n = 1	Q = 500 m³/s Veg = small D_{ch} = 100 m n = 1	
Type$_{veg}$	Q = 500 m³/s Veg = small D_{ch} = 100 m n = 1	Q = 500 m³/s Veg = large D_{ch} = 100 m n = 1	
D_{ch}	Q = 500 m³/s Type = small D_{ch} = 100 m n = 1	Q = 500 m³/s Type = small D_{ch} = 150 m n = 1	Q = 500 m³/s Veg = small D_{ch} = 200 m n = 1
n	Q = 500 m³/s Type = small D_{ch} = 100 m n = 1	Q = 500 m³/s Type = small D_{ch} = 100; 150 m n = 2	Q = 500 m³/s Type = small D_{ch} = 100;150; 200 m n = 3
PB	Q = 500 m³/s Type = small D_{ch} = 100 m n = 1 PB = ONE	Q = 500 m³/s Type = small D_{ch} = 100 m n = 1 PB = ALL	

As the meander evolves, the number of patches increases as well. The same simulations are carried out. However, in these simulations the number of patches, n, on the floodplain is varied for different hydrological conditions. Every simulation has a relating icon to quickly assess the type of simulation, which is visualized in Table 2-4. Lastly, vegetation on every pointbar (PB) shows the effects of multiple vegetated pointbars and is only simulated for the high flow conditions.

2.4. MONITORING AND EVALUATION

This section elaborates on the method of the data handling for further analysis. In this study, the results can be summarized in two-dimensional profiles and area ratios. The method to evaluate the results with these profiles and ratios is presented below.

2.4.1. TRANSVERSE AND LONGITUDINAL PROFILES

Three profiles are developed to allocate the along valley variations by the presence of vegetation of the velocity and the water depth, see Figure 2-5A). The red, blue and green lines show respectively the outerbank, the centreline of the channel and the upstream, downstream and in the vegetation patch. The upstream and downstream part of vegetation line is based on the average floodplain height of the vegetation patch. The longitudinal profiles change with the variation of position of the patch, whereas the outerbank and channel profiles are on a fixed place.

Additionally, five transverse profiles are shown in Figure 2-5B), perpendicular to the vegetation patch at the apex, examine the hydrodynamic changes. The transverse profiles located at the apex, the leading edge and the tailing edge examine the effects within the vegetation. Furthermore, upstream and downstream effects are studied in order to quantify the near-field variations in water level and velocity. The upstream and downstream profiles are shifted 20 meters upstream and downstream of the leading and trailing edge.
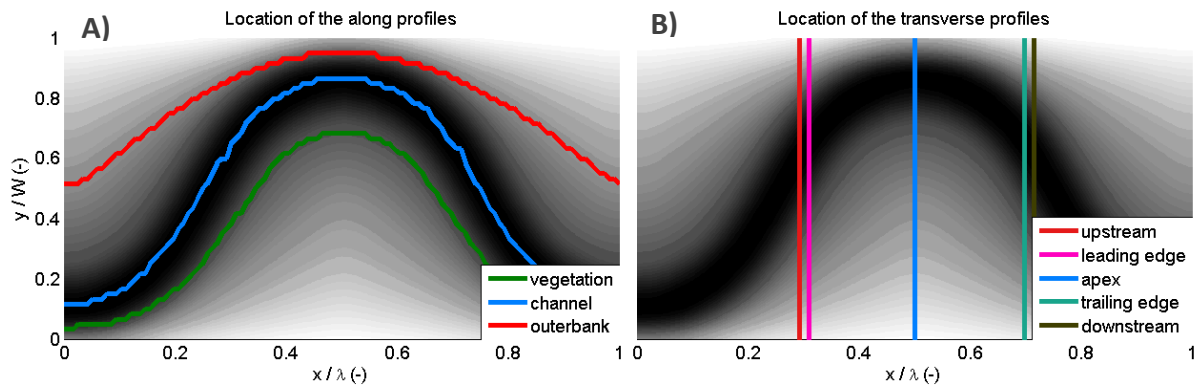
Figure 2-5 The results are examined by the longitudinal and transverse profiles. A) Definition of the longitudinal over the outerbank, through the channel and along the vegetation and B) transverse profiles at the apex within the vegetation patch (leading edge, apex and trailing edge) and near the patch (upstream and downstream).

2.4.2. AREA RATIO OF FLOODPLAIN FLOW

Due to the presence of the vegetation, the velocity in the arc of the patch will decrease. In order to compare the flow redirection over the floodplain by the various patch positions on the floodplain, a ratio is defined between the non-vegetated area of the relative decelerated flow velocity and the total non-vegetated area higher up the floodplain in the patch arc. The ratio will give an indication, whether the patch closes of the floodplain upstream (> ratio) or the redirection is strong enough to force the flow to go over the floodplain (< ratio). This flood redirection is important for the development of riparian vegetation on the floodplain behind the vegetation, as the water could disperse the seeds or set back the development in case of stronger flow velocities (< ratio). For a decrease in flow velocity, sedimentation patterns could stimulate the establishment of vegetation (>ratio). Furthermore, the morphological evolution of the meandering corridor is stimulated with higher flow velocities over the floodplain. With higher concentrated flow over the floodplain, cut-off events will occur more often (< ratio). Also the closing off of the floodplain by the presence of the vegetation patch can be determined. The ratio is used for the evaluation of high flood simulations, because the water can still flow on the inner arc of the patches higher up the floodplain.
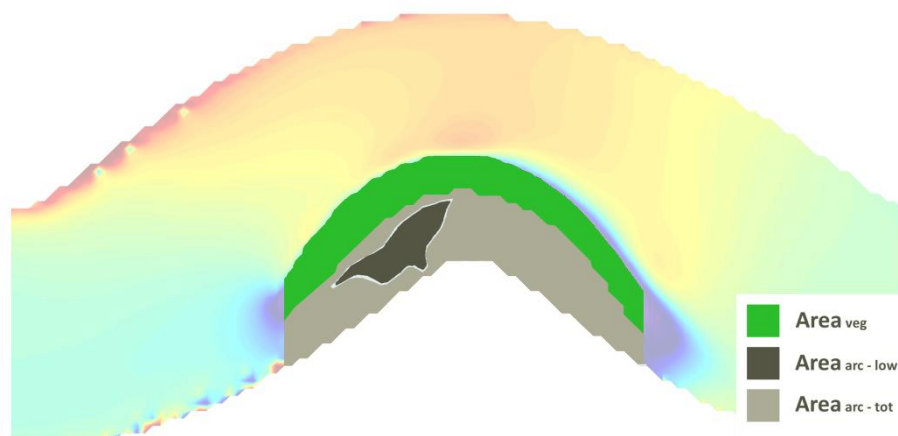
Figure 2-6 Definition of the ratio between the area of decelerated flow and total area under the vegetation patch. This ratio indicates the rate of closure upstream by the vegetation patches, based on the redirection of the flow over the floodplain.

2.4.3. THE BLOCKAGE FACTOR

The blockage factor is used to analyse the distribution of the discharge. Discharge over the floodplain and through the main channel at the apex defines this distribution, see Equation 2-9. For the channel definition, see

. The relative discharge distribution (α) between the channel (Q_{ch}) and the floodplain (Q_{fl}) is defined as follows:
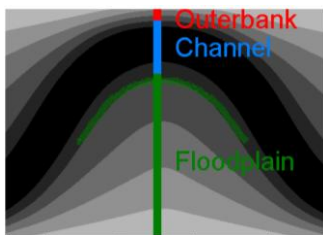
$$\alpha = \frac{Q_{fl}}{Q_{ch}}$$

Equation 2-9

Figure 2-7 Definition of the floodplain and the channel in order to define the discharge distribution (α).

The blockage factor is used as an indicative variable to explain to hydrodynamic effects at a reach scale. This geometric description is based on the work of Green (2005a). The blockage (B_x) is the ratio between the area covered by vegetation (wh) and the cross-sectional wetted area of the channel (WH). In order to quantify the validity of the relation between the blockage and the distribution of discharge, the coefficient of determination (R^2), is used for the different hydrological conditions.
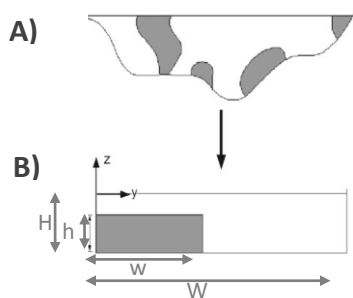
$$B_x = \frac{wh}{WH}$$

Equation 2-10

Figure 2-8 Schematic definition of the blockage by vegetation patches. A) Cross-sectional view with vegetation and B) the mathematical vegetation description in order to define the blockage factor by vegetation (Luhar et al., 2008).

3. RESULTS AND INTERPRETATION

In this chapter, the results of the simulations in the hydraulics module of Delft3D is presented and interpreted. The model set-up is defined by a large number of parameters and variables. This study focuses on the varying positions of vegetation patches. During the systematic approach all parameters are kept constant in a controlled environment, except the vegetation patch characteristics. The control run without vegetation serves as a reference to the simulations with vegetation patches. Analyses of the results are based on the changes in water level, relative velocity and discharge distribution over the floodplain.

Results of the hydrodynamic effects caused by the presence of a single vegetation patch on the floodplain are discussed in the first section, where small vegetation under high discharge conditions is presented. Secondly, the results of the variation in position of the vegetation patches under different hydrological conditions are presented. Thirdly, the results of multiple vegetation patches are presented. Finally, all simulations are combined to explain the discharge distribution over the floodplain by the blockage at the apex.

3.1. SINGLE VEGETATION PATCH

In this section the control simulation is compared to a simulation with one vegetation patch near the channel under high discharge conditions. The patch is located at 100 meter from the channel, which is defined as the median water line. The patch consists of homogeneous vegetation, which is presented in Table 2-2. The shape of the patch follows the water line, as seen in nature. Figure 3-1 shows the control and a single vegetation patch simulation for a high flood event.

The presence of a vegetation patch leads to set-up of water, where the set-up propagates several 100's of meters upstream with the strongest increment in the order of several centimetres at the leading edge of the vegetation patch, shown in Figure 3-1C). An increase in water level at the leading edge increases the initial inundation of higher floodplain area. Furthermore, the water set up is larger higher up the floodplain at the inner curve of the vegetation patch relative to the outer curve, as the vegetation catches the water upstream. Finally, there is a wake, with a decreased water depth downstream of the vegetation patch as a result of the blockage by the vegetation.

The lower velocity induces the set-up of water and increases the residence time within the vegetation. Figure 3-1D) and E) show respectively the magnitude and direction of the flow for the control and the single vegetation patch simulation, where the differences are visualized in F). A strong reduction of flow velocity is visible, with a mean flow velocity reduction of 0.24 m/s within the patch. The maximum absolute flow velocity reduction is located just after the apex of the meander bend. As water is partly blocked by the patch, the vegetation forces more flow to go around the patch, which is visible by the reduction in flow velocity at the location of patch. The increased velocity in the channel and the non-vegetated floodplain could strongly increase erosion near the vegetation patch. The increase in velocity in the channel enhances the migration rate of the meander bend, whereas increase of flow velocity on the higher part of the floodplain can stimulate a cut-off event. Lastly, the velocity reduction propagates more downstream than upstream, which is visible at the trailing edge of the vegetation patch.
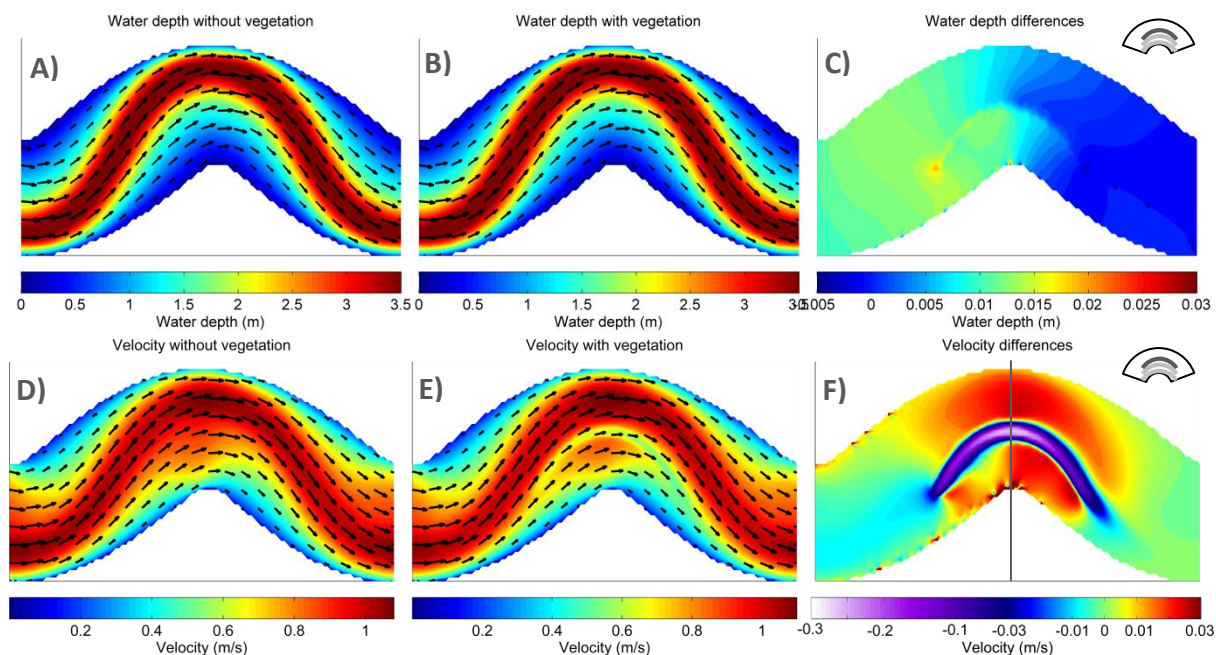
Figure 3-1 Water depth and velocity changes as a results of the presence of a single vegetation patch during a high flood event. A) The water depths for the control simulation. B) The simulation with vegetation and C) the absolute water level changes. D) The velocities for the control simulation. E) The simulation with vegetation. F) The absolute velocity changes, whereby one should take note of the double linear scale bar. The small arrows in A), B), D) and E) indicate the velocity magnitude and the direction of the flow.

3.2. POSITIONING OF A SINGLE VEGETATION PATCH

This section compares the results of simulations with vegetation situated at 100, 150 and 200 meter from the channel. The increase in water depth and flow accelerations and decelerations are studied under various hydrological conditions and different types of vegetation, small and large. The plan views of the water depth change in all simulations are given in Appendix I and the overview of the results of the changes in the magnitude of the velocity is given in Appendix II. The transverse and longitudinal profiles are shown in Appendix III.

3.2.1. WATER LEVEL CHANGES FOR DIFFERENT POSITIONS

The location of maximum water set up upstream of the vegetation patch does not change for variation in the location of the patch. Figure 3-2 shows the differences for three positions of the vegetation patches for large vegetation with a high flood event.

For the medium flood event, the vegetation has a large effect near the channel and an almost non-existent effect relatively far from the channel. The location of the vegetation has relative small effect for the high discharge simulations. However, as the vegetation patch approaches the water line higher up the floodplain, the absolute reduced water level behind the vegetation is more pronounced. It covers a larger area and has a higher magnitude.

The water level change within the arc of the vegetation patch propagates more downstream relative to the outer curve on the floodplain or channel for all three simulations. The downstream propagation within the vegetation patch arc is strongest for vegetation patches closest to the channel, as the vegetation patch closes of the floodplain. Lastly, patches closest to the channel clearly result in the highest water level increase at the leading edge. However, the water set up for small vegetation under high flow conditions is strongest at 150 meters. At this location the rate of submergence is close to one.
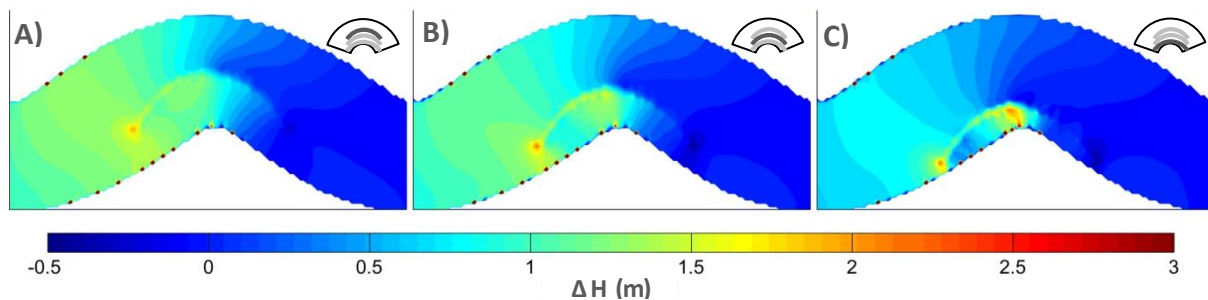
Figure 3-2 Plan view of absolute water level changes for various positions of the vegetation patch on the floodplain for high discharge conditions and small vegetation. A) Vegetation patch close to the main channel, B) middle on the floodplain and C) close to the water line. A patch closer to the channel raises the water level stronger in the channel. However, the patch highest up the floodplain shows stronger near-field effects.

3.2.2. FLOW VELOCITY CHANGES FOR DIFFERENT POSITIONS

The relative velocity change within the vegetation is largest for the average flow condition relative to the high discharge. The vegetation patch is relatively close the channel, see A). The flow for the average flow condition is mainly redirected through the main channel, because the morphology and the vegetation prevent more flow over the floodplain, whereas the flow under high discharge conditions can still go around the vegetation over the floodplain. The reduction within the vegetation is also largest for the simulation for the largest distance between the patch and the channel, shown in C). The vegetation closes off the floodplain and the height of the vegetation relative to the water depth approaches 1. The velocity at the outer bank perpendicular to the leading edge of the vegetation patch increases in all simulations. While the maximum relative increase in velocity in the main channel for the varying positions of the vegetation is mostly located around the apex of the meander. To further explore these velocity changes, transverse and along stream profiles are discussed.

The magnitude of the relative velocity change at the trailing edge is larger in comparison with the leading edge, as shown in Figure 3-4. Furthermore, the change in velocity is largest at the apex of the meander bend within the vegetation. As the patch changes position on the floodplain, the relative velocity decreases from 0.28 to 0.57 within the patch. The relative flow changes at the leading and trailing edges show even a larger relative decrease for a varying position, which is consistent throughout all the simulations, see Appendix III. Besides the relative decrease in velocity within and close to the vegetation (<20m), the relative velocity also increases at the edges, which is a result of the closing off of the floodplain. Depending on the position of the patch, either the redirection of the flow is dominant through the channel or over the higher non-vegetated floodplain. As a higher position closes off the floodplain, the velocity strongly accelerates at the edges, which is shown by a decrease within the patch and acceleration at the edge for the leading edge in Figure 3-4C).
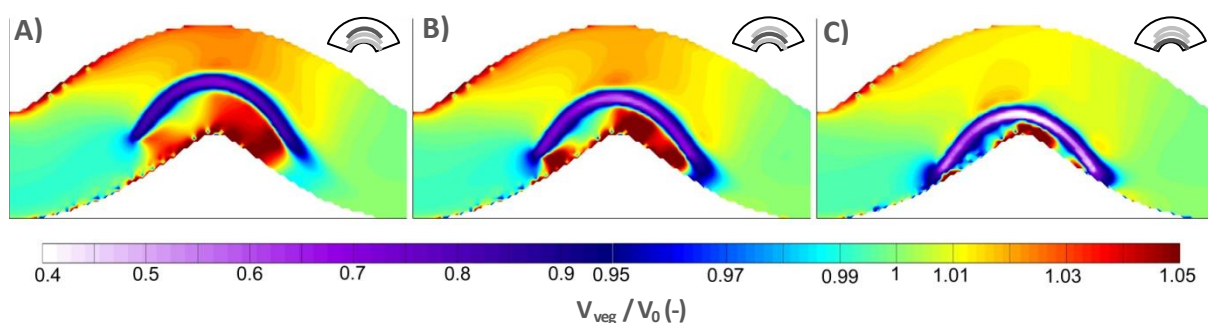
Figure 3-3 Plan view of normalized velocity changes for various vegetative patch positions on the floodplain for a high flood event and small vegetation. Vegetation closest to the water line shows highest near-field effects, whereas patches close to the channel accelerate more flow to the channel. Note the double linear scale bar.
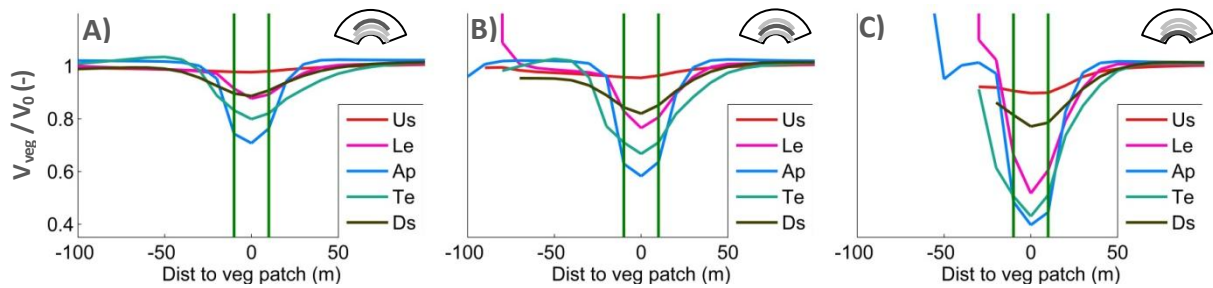
Figure 3-4 Transverse normalized velocity profiles for various vegetative patch positions shows a stronger deceleration for the edges of the patch relative to the apex. The green lines indicate the position of the vegetation and the coloured lines show the transverse profiles of upstream (Us), leading edge Le), Apex (Ap), Trailing edge (Te) and downstream (Ds) of the vegetation. A positive distance to vegetation patch indicates less distance to the main channel.

The relative velocity change in the patch increases as the patch moves higher up the floodplain, which is shown in the longitudinal profile in Figure 3-5. However, the relative velocity changes at the leading edge and the trailing edge increases relatively much more compared to the changes at the apex and a triple peaked pattern arises, shown in Figure 3-5C). A similar pattern is confirmed for other simulation, although sometimes only a double peak is visible for the medium flood. This can be explained by the closing off of the floodplain area behind the patch, which concentrates the flow higher up the floodplain. The water is also redirected through the channel and over the outerbank, mainly upstream relative to the patch location, but this redirection through the channel does not vary as the position of the patch changes. Lastly, the hydraulic downstream lag at the apex does not shift and the relative increased velocity at the outer bank does not change.

The closing off of the floodplain by a higher position of the patch is reconfirmed by the area ratio of deceleration, which is shown in Figure 3-6. This area ratio shows the flow diversion on the floodplain and is defined in Figure 2-6. Vegetation higher on the floodplain has relatively more area with a deceleration compared to the total non-vegetated area in the arc of the vegetation patch. Furthermore, the flow is strongly redirected for large vegetation near the channel and more than 95% of the area below the vegetation patch has an accelerated flow relatively to the control simulation. The patches higher up the floodplain are closer to the waterline and the arc closes off the floodplain and result in an increase in the decelerated area ratio. This deceleration of flow could stimulate sedimentation behind the vegetation patch. The location of the deceleration in the arc is mostly found between the leading edge and the apex of the patch.
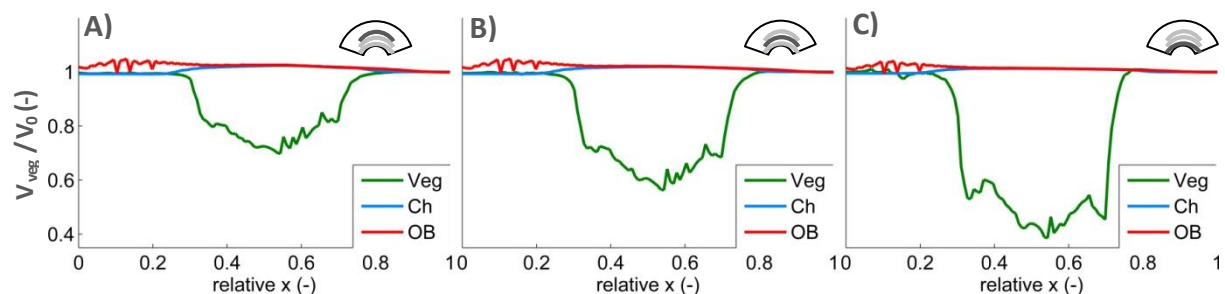
Figure 3-5 Longitudinal normalized velocity profiles for various vegetative patch positions show a stronger deceleration at the leading and trailing edges for patches higher up the floodplain, which results in the triple spiked pattern. The coloured lines indicate the position of the profiles of the vegetation, channel and outer bank.
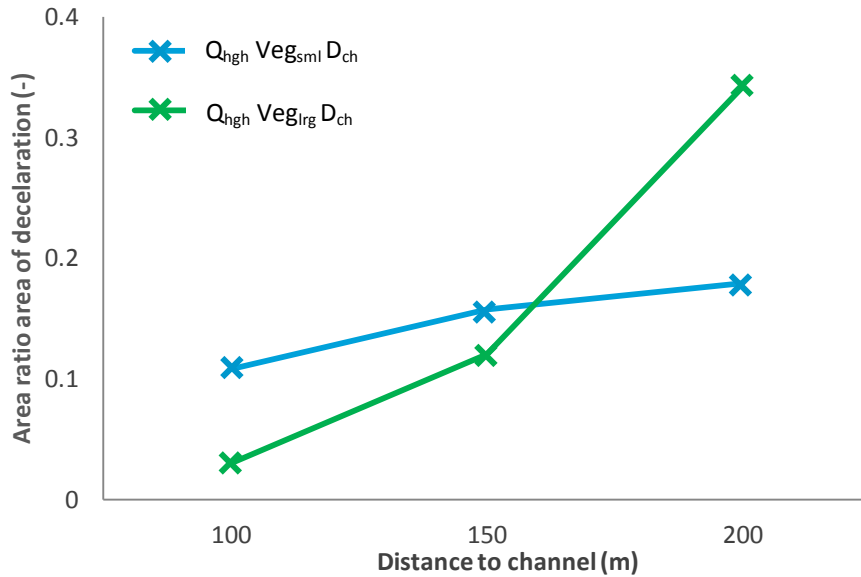
Figure 3-6 Increase in the distance from the channel increases the relative area with a deceleration of flow velocity higher up the floodplain compared to the control simulation for a high flood event. The response of varying the distance on the deceleration of flow on the floodplain is strongest for larger vegetation (Veg$_{lrg}$) relative to small vegetation (veg$_{sm;}$) and indicates closing off of the floodplain upstream.

3.3. MULTIPLE VEGETATION PATCHES

The hydrodynamic effect of the location of the patch also depends on its local surroundings, such as the presence of other vegetation patches, which can stimulate flow between the patches or act as one patch. This section presents the results of simulations with one, two or three vegetation patches at respectively 100, 100 and 150 and 100, 150 and 200 meters from the channel. The effects are studied for medium and high discharge conditions and small and large vegetation patches. Firstly, the water level and velocity changes are described. Thereafter, the local flow redirection over the floodplain is described.

3.3.1. WATER LEVEL CHANGES FOR MULTIPLE VEGETATION PATCHES

Multiple vegetation patches induce a cumulative water set up in front of the vegetation patches, see Figure 3-7 for water level changes for 1, 2 and 3 vegetation patches for small vegetation with a high flood event. The same water level change patterns arise, which are discussed for in the single vegetation patch section, such as a wake behind the patch and a increase in water depth the leading edge. This section focuses on the alternation of the hydrodynamic effect by the variation of the number of patches.

The water level rise is also largest at the leading edge for multiple vegetation patches. However, a cumulative rise at the beginning of the floodplain is induced by the presence of multiple vegetation patches, which enables flow to pass easier over the higher floodplain behind the vegetation patch. A steeper gradient between the water level change in the arc of the patch and the depression wake behind the vegetation is the result of simulations with more patches, as shown in Figure 3-7.
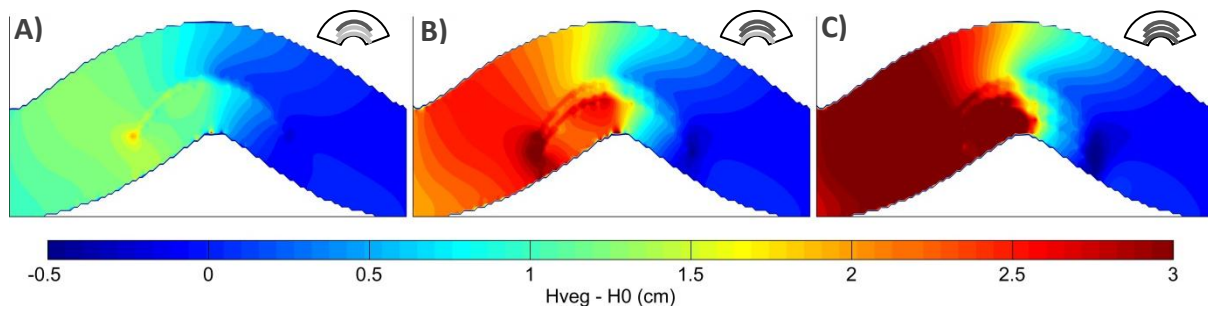
Figure 3-7 Plan view of absolute water level changes for A) one, B) two and C) three patches on the floodplain for high discharge and small vegetation. The water level rise increases cumulatively and is largest at the leading edge for all simulations. This enables water to flow over the floodplain and vegetation, in case of submerged vegetation, with less resistance.

Furthermore, the depression area with negative water level changes downstream of the vegetation enlarges as more patches are present in the wetted cross-sectional channel area, as well as the largest water depth in the respective area. The wake behind the vegetation does not change its position. The water level changes between the patches for all simulations are lower relative to water level changes in the surrounding vegetation patches, which indicate a stabilization of flow between the patches. Furthermore, the downstream water level adaption within the arc moves from near the patch for A) to closer to the floodplain boundary in B) and C).

3.3.2. FLOW VELOCITY CHANGES FOR MULTIPLE VEGETATION PATCHES

The flow diversion on the floodplain is stronger in the vegetation patch, over the floodplain and in the channel as more vegetation patches are present on the floodplain. Figure 3-8 shows the relative velocity change for multiple vegetation patches with a high discharge condition and small homogenous vegetation patches. The flow velocity accelerates strongly in the arc of the vegetation patch as the distance between the patch highest on the floodplain and the water line decrease, even though the relative flow velocity at the leading edge decreases strongly for multiple patches. Furthermore, the flow velocity in the channel and at the outerbank increases strongly for more patches, which indicates the presence of more blockage by vegetation stimulates the secondary flow pattern in a meander bend.

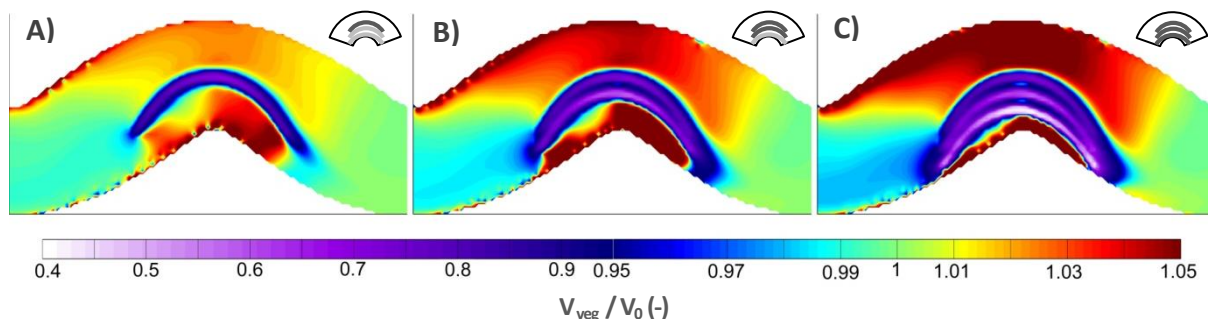**Figure 3-8 The relative flow velocity increases at the outerbank and in the channel for more patches, which is shown by the plan view of normalized velocity changes for various number of vegetative patches on the floodplain for a high flood event and small vegetation.**

The distance between the vegetation patches relatively to the width of the patch does not stimulate water to flow between the patches in these simulations, see Figure 3-9. However, they are not behaving as one patch either. In that case, the flow would be forced to go around the vegetation patches and the velocity change would decelerate strongly between the vegetation patches at the apex (Temmerman et al., 2007). In Figure 3-9A) the centre of the patch at 100 meter from the channel is located at zero meters. This patch does not change from position for the three simulations in this graph. A larger negative distance to the vegetation patch nearest to the channel represents a location higher up the floodplain, whereas a positive distance represent a location nearer to the channel on the lower part of the floodplain. The relative flow velocity between the patches at the apex approaches 1, which indicates the flow between the vegetation patches does not accelerates or decelerates relative to the control simulation, see B). This is also indicated for a third vegetation patch, which shows a consistent pattern. The relative flow velocity to the control simulation also approaches one, see C). The average relative velocity between all patches, for various discharge conditions and vegetation types between two vegetation patches is 0.91. However, the flow is more strongly decelerated between the patches up- and downstream compared to the flow between patches at the apex.

An additional vegetation patch increases the flow velocity within other patches relative to the simulation with one patch. For the single patch simulation, the flow diversion is clearly visible with higher flow velocities around the vegetation and a strong flow velocity reduction at the location of the vegetation patch. This flow diversion is redirected to other patches nearby and results in an increase of the decelerated flow within the patch at the apex, see the arrow in Figure 3-9. The simulations with large vegetation also show an increase of relative flow velocity in the patch compared to the simulation with a single vegetation patch, see the small grey arrows in Figure 3-9.

Instead of an increase in decelerated area by closing off the floodplain for patches higher up the floodplain, multiple patches mainly accelerate the flow over the higher floodplain, see Figure 3-10. Especially for smaller vegetation, more patches on the floodplain result in a smaller area with deceleration behind the patch. For tall vegetation the relative area slightly increases. The relative decelerated area for multiple patches never extends 10% of the total area behind the arc of the patch, which indicates flow acceleration over the floodplain. The concentration of flow over the floodplain stimulates channel formation and can lead to a cut-off event. The development of the patch itself could be stimulated by seed dispersal further on the floodplain as a result of the higher flow velocity. However velocity exceeding uprooting levels could set the development back.
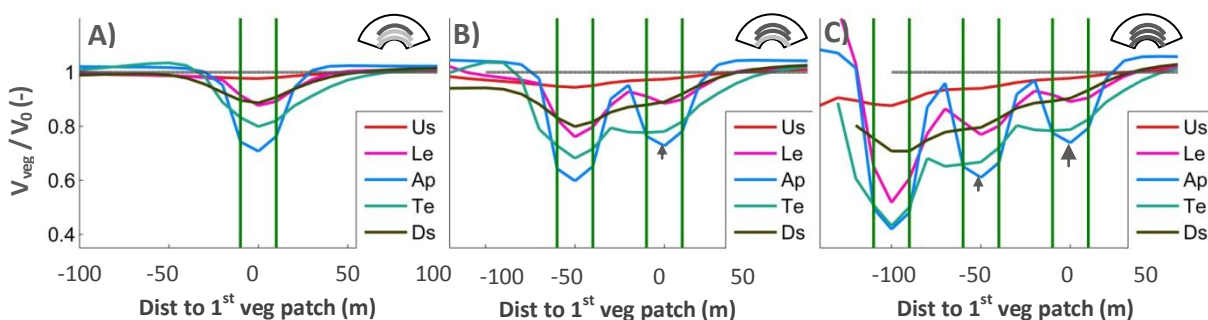
Figure 3-9 Transverse normalized velocity profiles for a various number of vegetation patches of the small vegetation type. The flow velocity at the apex shows almost no change, which indicates the width relative to the distance between the vegetation patches is near equilibrium. The green lines indicate the position of the vegetation and the coloured lines show the transverse profiles of upstream (Us), leading edge (Le), Apex (Ap), Trailing edge (Te) and downstream (Ds) of the vegetation.
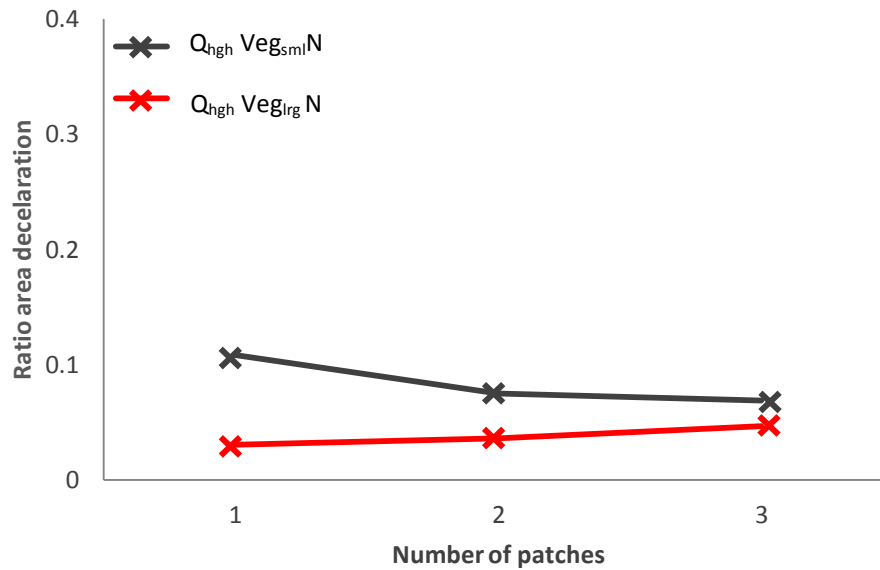
Figure 3-10 More vegetation patches higher up the floodplain decreases the relative deceleration flow area in the arc of the patch compared to the control simulation. This indicates flow concentration over the floodplain between the water line and the patches and can lead to channel development on the floodplain.

3.4. BLOCKAGE BY VEGETATION PATCHES IN A MEANDER REACH

This section combines the simulations with variation in patch position, number of vegetation patches, hydrological conditions and vegetation type into a blockage factor at the apex. Thereafter, the blockage is related to the distribution of discharge in a meandering system. But first of all, the change in water level and velocity for the various locations and the number of patches is compared, which is described by the Chézy number for the whole reach. Thereafter, the variation in variables is related to the redistribution and lastly, the distribution is explained by an overall blockage factor at the apex.

3.4.1. COMPARE VARIATION IN DISTANCE TO CHANNEL WITH NUMBER OF PATCHES

The downstream boundary of the simulation, located after the 7th meander, forces flow at a predetermined water level in the model. The water levels of the simulations with placement of vegetation patches on all point bars are shown in Table 3-1 under the different hydrological events. The hydraulic response also includes the blockage by the vegetation and the cross-sectional coverage, which excludes the density of the vegetation. The maximum local set up of water level in front of the patch is 7 cm for three patches with large vegetation on the floodplain under high discharge conditions inducing an average 2.0% rise at the reach scale. The water rise and the reach-averaged velocity can be related to Chézy's coefficient. The volumetric blockage and the cross-sectional coverage by vegetation also depend on the hydraulic situation as the water level changes.

The water set up is strongest upstream of the apex and the velocity decelerates most within the vegetation. Distinction in these four locations partly explains the change in water depth and flow velocity, see Figure 3-11. However, still some overlap between the location clusters occurs. The absolute velocity and water level changes are shown for one meander wavelength, which includes the channel and outerbank. The simulations represent variations in distance of the patch to the channel and the number of patches with a discharge of 500 m³/s. Furthermore, upstream and downstream are defined relative to the apex of the meander. Simulations with multiple patches show occurrence of lower flow velocities downstream and upstream in the non-vegetated areas, which are located between the patches, as well as a strong increase in the water level rise. The hydrodynamic responses of the medium discharge condition and the tall vegetation are given in Appendix IV. Scatters plot with a lower amount of points indicate less change, as points collide for the same hydrodynamic conditions relative to the control simulation.

Table 3-1 Overview of the results for simulations with variations in number of patches and distance to the channel for various vegetation types under two flood events. The reach-averaged hydraulic response is presented with velocity, Chézy's coefficient. Also the volumetric blockage and the coverage at the apex are presented.

| Serie	Simulation variables				Hydraulic response			
	n (-)	D_{ch} (m)	$Type_{veg}$ (-)	Q (m^3s^{-1})	$\bar{u}$ (ms^{-1})	C ($m^{1/2}s^{-1}$)	Blockage (m^3m^{-3})	$Coverage_{veg}$ (m^2m^{-2})
Control 01	0	-	-	med	0.63	19.9	0.0%	0.0%
Control 02	0	-	-	high	0.73	20.8	0.0%	0.0%
N 1a & Dch 1a	1	100	sml	med	0.61	19.1	1.1%	8.3%
Dch 1b	1	150	sml	med	0.62	19.3	0.4%	3.3%
Dch 1c	1	200	sml	med	0.63	19.9	0.1%	0.8%
N 2a & Dch 2a	1	100	sml	high	0.72	20.6	0.7%	5.0%
Dch 2b	1	150	sml	high	0.72	20.4	0.7%	5.0%
Dch 2c	1	200	sml	high	0.71	20.2	0.6%	4.8%
N 3a & Dch 3a	1	100	lrg	med	0.61	19.2	0.8%	3.3%
Dch 3b	1	150	lrg	med	0.62	19.6	0.2%	1.0%
Dch 3c	1	200	lrg	med	0.63	19.9	0.1%	0.3%
N 4a & Dch 4a	1	100	lrg	high	0.71	20.3	1.0%	4.3%
Dch 4b	1	150	lrg	high	0.71	20.2	0.7%	3.0%
Dch 4c	1	200	lrg	high	0.72	20.4	0.4%	1.7%
N 1b	2	100, 150	sml	med	0.61	19.1	1.5%	11.8%
N 1c	3	100, 150, 200	sml	med	0.59	18.6	1.6%	12.6%
N 2b	2	100, 150	sml	high	0.72	20.6	1.3%	9.9%
N 2c	3	100, 150, 200	sml	high	0.71	20.2	1.9%	14.8%
N 3b	2	100, 150	lrg	med	0.61	19.2	1.0%	4.3%
N 3c	3	100, 150, 200	lrg	med	0.60	18.9	1.1%	4.6%
N 4b	2	100, 150	lrg	high	0.71	20.3	1.7%	7.3%
N 4c	3	100, 150, 200	lrg	high	0.69	19.7	2.1%	9.0%
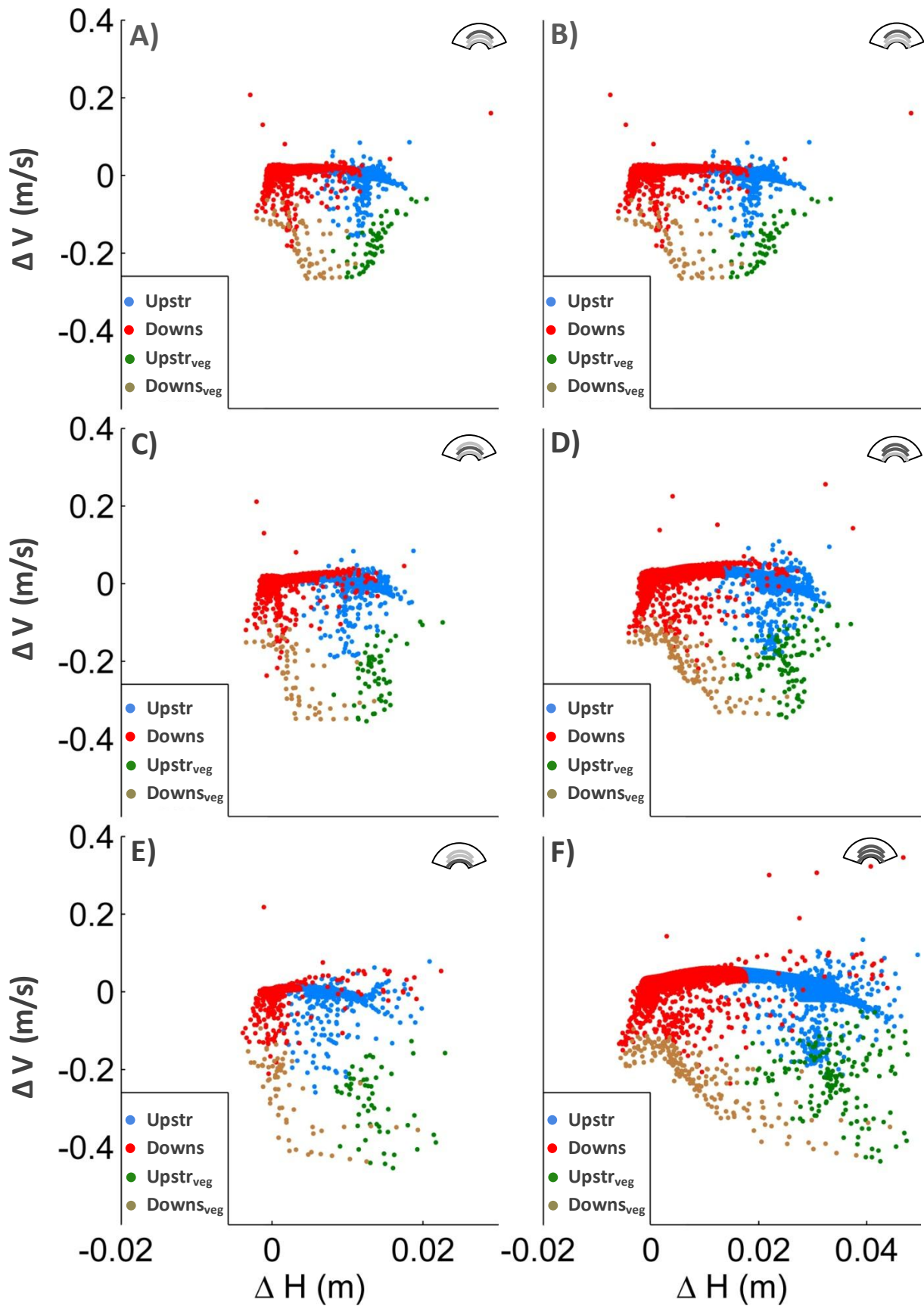
Figure 3-11 The changes in water depth and velocity depend on the location relative to the patch and the meander apex. Six simulations are presented for a single meander wavelength with high discharge and small vegetation. The colour indicates the position on the meander reach.

This study simulates steady open channel flow, where the Chézy's coefficient can describe the resistance and is used to quantify the hydraulic effect of the presence of vegetation patches for the whole reach, where the computation of the Chézy's coefficient is shown in Equation 2-1. The average resistance coefficient for the river reach is determined for all simulations and is shown in Figure 3-12. Without vegetation, the average reach scale Chézy coefficient is 22.9 and 24.4 m$^{1/2}$/s for respectively 90% and 99% occurring flood event. Higher discharge encounters less resistance by the bed and vegetation and results in a higher coefficient. As more vegetation is present in the reach, the blockage factor in the reach increases. The blockage factor represents the ratio between the area of vegetation in the channel and the wet cross section at the apex. Further details on the blockage factor are shown in Equation 2-10. An increase in the blockage factor at the apex results in a higher average resistance for the river. The rate of resistance increase by the blocking vegetation is similar for the hydrological conditions with these relative low blockage factors.

The geometrical variables clarify the discharge distribution at the apex to a large extent, shown in Figure 3-13. In Figure 3-13A) the increased distance to the main channel relates to a higher overbank flow. The vegetation patch near the main channel effects the redistribution of the flow strongest. However, the vegetation patch in the middle at 150 meter from the channel has the strongest effect on the flow distribution with the high discharge condition. The rate of submergence of the vegetation in the wetted area is of importance in order to explain the redistribution of flow. This is also indicated by the number of patches, however indirectly. The magnitude of change in redistribution between one and two vegetation patches is larger in relation to two and three vegetation patches for the high discharge condition. Simulations with a medium discharge and multiple vegetation patches lower the increment of distribution magnitude, as the patches close in on the water line.
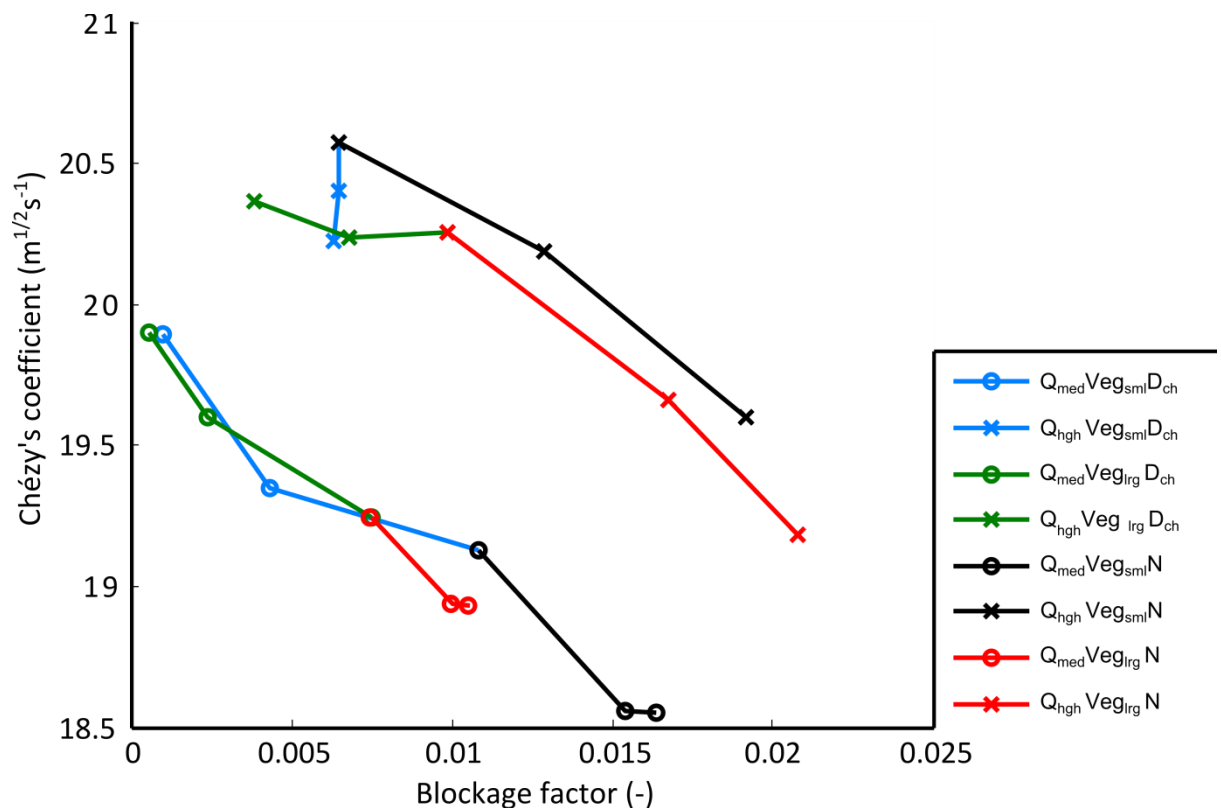

Figure 3-12 The higher vegetation blockage at the apex results in more resistance in the river reach. The reach-averaged Chézy's coefficient represents the resistance of the simulation. Please note the consistent use of colour and symbology throughout the following results, which represent a series of simulations.
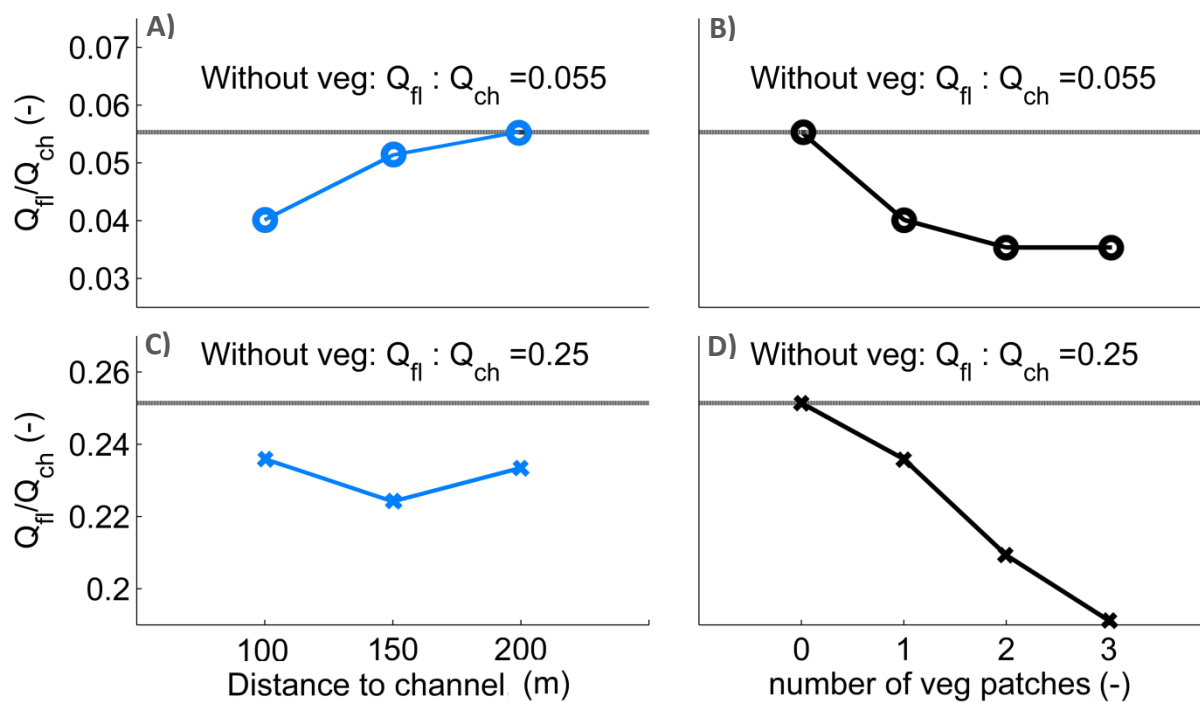
Figure 3-13 The magnitude of discharge redirection at the apex is largest for the submerged vegetation patch in the middle. The horizontal line indicates the discharge distribution in the control simulation without vegetation. A) shows three simulations with various patch positions relative to the channel for medium discharge B) various number of vegetation patches. C) and D) similar only for the high flood event. The presented simulation series is for small vegetation.

3.4.2. BLOCKAGE FACTOR FOR ALL SIMULATIONS

The blockage, defined in section 2.4, explains the discharge distribution at the apex for the various hydrodynamic conditions, see Figure 3-14. The discharge distribution is the ratio between the discharge over the floodplain and through the channel, which is 0.055 and 0.25 for respectively the 10% and the 1% occurrence flood events without vegetation. The simulations with various types and numbers of vegetation patches, with differences in distance to the channel create a variety of blockage at the apex. This explains the discharge distribution for medium and high flow condition of respectively 98% and 92%. The symbol in Figure 3-14 indicates the flood condition. A line with a specific colour and the same symbol represents a range of three simulations with a varying vegetation type and either a change in the distance to the channel or the number of patches. The blockage always increases for the number of patches. However a patch with a larger distance to the channel does not necerally increase the blockage, because of the rate of submergence, as discussed above. With the steep gradient and the starting distributions of flow for each hydrological condition, there would be no flow with a blockage of 4% and 7% for respectively the medium and high flow. The structural density of the vegetation is 23% and 13% for small and large vegetation stands, see Table 2-2. Therefore the simulations have an actual coverage area by the vegetation on the floodplain between 0 and 58% and the density of the vegetation determines the maximum blockage for the an entire vegetated floodplain.

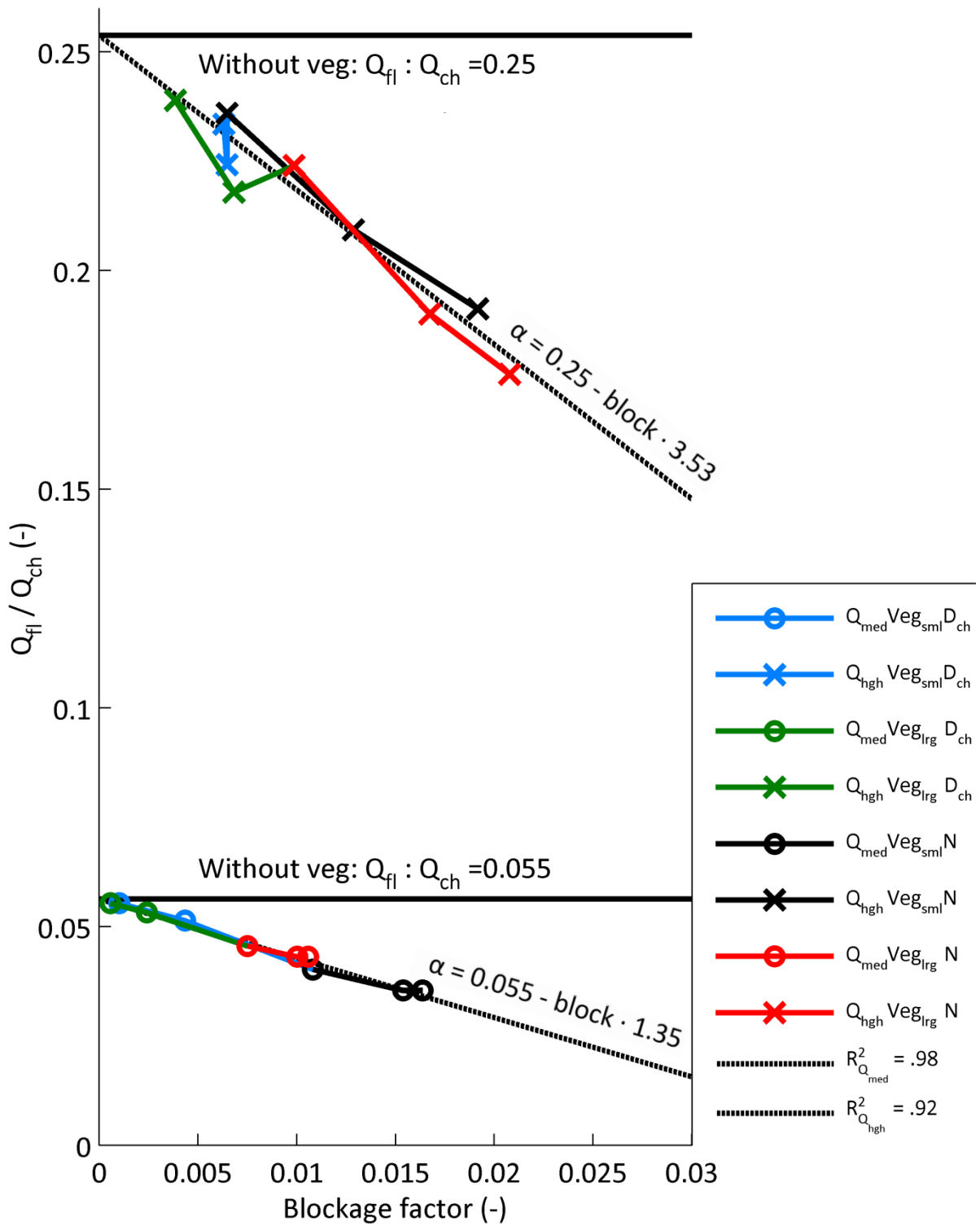**Figure 3-14 Blockage induced by various positions of vegetation patches clarifies the discharge distribution for two hydrological conditions. The simulations with various positions and number of patches with two vegetation types are all included to determine the reach scale response by the presence of the patch. The lower and upper trend lines are respectively for the medium and high flood event.**

A higher blockage by the vegetation on the floodplain shows a reduction in overbank flow as presented in Figure 3-14. The flow is redirected to the channel and the outerbank. Although the coefficient of determination shows good agreement, some variance is still unexplained. Instead of an increase in decelerated area by closing off the floodplain, multiple patches mainly accelerate the flow over the higher floodplain, which is shown in Figure 3-10. In order to support this, Figure 3-15 shows the variance of the simulated discharge distribution and the corresponding trend line. An increase in the number of vegetation patches shows a higher rate of redirected flow to the channel instead of floodplain overflow, thus implying a higher blockage on the floodplain. This can be explained that the flow between patches is blocked by the turbulences occurring on the edges of the multiple patches. These turbulences between the patches are mainly decreasing the relative velocity at the leading edge and the trailing edge, as shown in Figure 3-9B) and C). Only the simulation with large vegetation under high discharge conditions shows a deviant pattern The number of patches in this simulation actually lowers the redirection of flow to the channel relative to the trend line, which is yet unexplained.
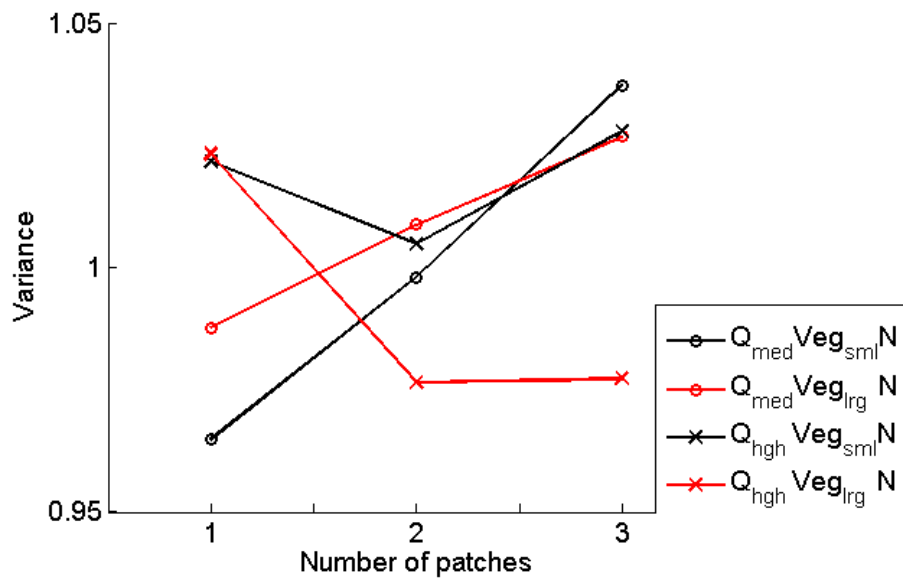

Figure 3-15 The flow between patches partly explains the variance between the trend line and flow distribution. Flow between the patches is decelerated by turbulences on the edges of the patches, which tend to behave as one patch at the leading and trailing edge and therefore redirect the flow over the floodplain.

4. DISCUSSION

The discussion presents the general implications of the hydraulic effects found in the simulations with the systematic variation of vegetation patch position. Furthermore, the possible sensitivities of the results are discussed, which covers the hydraulic implementations of the real-world complexity of vegetation and meander dynamics in relation to the results found in simulations in this study. Lastly, the results are compared to work of others, which can be found in literature.

4.1. DISCUSSION OF METHODS

4.1.1. INDIVIDUAL CHARACTERISTICS OF VEGETATION

Firstly, the vegetation description by Baptist et al. (2007) simplifies the vegetation as rigid cylinders, which tends to overestimate the flow in the vegetation. This is mainly caused by ignoring the complex physical characteristics of vegetation, such as bending, waving and foliage (Järvelä, 2002; Ghisalbert and Nepf, 2009). Underestimation of flow reduction results in higher simulated flow velocities within the vegetation patches, as well as a lower water set-up at the leading edge and less flow diversion in the channel as presented in the simulations.

Furthermore, the implementation of vegetation in grid cells of 10*10m is reasonable for the river Allier case, where distinctive arc-shaped patterns of Salix are observed. However, smaller scale vegetative objects were also found, which alter the near-field effects on the vegetation patches. For example dead wood debris and the related morphology around this debris can result in noticeable effects in river reach scales (Gurnell et al., 2012). Therefore the found near-field effects are only describes the hydraulic response within a range of 10's of meters.

4.1.2. POSITIONING OF THE VEGETATION PATCHES

The varying position of the vegetation patch simulates the various positions of meander bends. These meander dynamics are strongly simplified in this study. The position of the main channel relative to the vegetation patch moved one-directional, namely perpendicular of the flow direction. This simulates the bend expansion of the meander, but the meander bend also migrates downstream and grows into a more asymmetrical bend (Seminara et al., 2001). The downstream migration affects the blockage of the vegetation patch, because the patch will be positioned relatively more at the leading edge of the pointbar, see Figure 1-1D). The older vegetation patches are located on the leading edge and the apex, whereas the younger stands are more located on the apex and the trailing edge.

The verification of the vegetation location is based on the habitat suitability index (HSI), which depends on the days of inundation per year (Duel and Specken, 1994), although it is known from literature that riparian vegetation self-organizes and reinforces its own habitat and does not solely depend on the hydrological conditions (Schoelnyck et al., 2011). Several studies advocate other suitability variables for riparian vegetation. Vreugdenhil et al. (2006) show the relative dominance of flood duration, –frequency, and –depth on the presence of riparian saplings in fluvial systems. For the Populus Nigra, the total inundated days per year was most dominant indeed. However for other riparian vegetation types, e.g. the Salix Alba, the average duration of a flood event and the inundation depth is far more important relative to the inundation period per year. Besides the hydrological connectivity, also the soil and temperature conditions control the vegetation development (Tabacchi, 1998). Nevertheless the verification, based on the total inundated days per year, shows good agreement with the creation of vegetation structures in a meander reach and supports the positioning on the floodplain.

4.1.3. DETERMINATION OF FLOW DIVERSION

To determine the flow diversion, two indicators are used in this study. Firstly, the relative area of decelerated flow within the arc of the patch is used. This indicates if the floodplain is closed off by the presence of the vegetation patch or if it actually accelerates the flow in the inner bend stimulating channel formation.

Secondly, the discharge distribution at the apex between the channel and the floodplain is used to study the redirection into the channel. The results depend on the definition of the floodplain, which in this study is based on the 50% occurrence flood event for the Allier. This can make it harder to compare to other studies, although the reach average Chézy's coefficient or other comparable reach-averaged resistance variables are an often used variable to compare the effectiveness of vegetative patches to redirect the flow (e.g. Green, 2005a; Luhar and Nepf, 2013).

4.2. DISCUSSION OF RESULTS

4.2.1. HYDRAULIC RESPONSE WITHIN AND NEAR THE PATCH

The largest water depth change as a result of simulations with vegetation is located at leading edge, the entrance region. This is in accordance by various authors (e.g. Nepf, 1999; Sinichalchi et al., 2012). The increasing flow depths enhance the flooding risk of the downstream floodplain as the water flow encounters less resistance with a larger flow depth. The higher upstream overbank flow in meandering systems can lead to faster channel migration due to cut-off events relative to less overbank flow and increase the rate of meander evolvement (Van Dijk, 2013).

The position of the largest reduction of flow velocity, however, varies from literature. Sinischalchi et al. (2012) shows the largest reduction at the leading edge of the vegetation patch in a small scale experiential set-up in a straight laboratory flume. In contrast, the largest velocity reduction in this study within the patch is approximately 10-20 meter after the apex of the meander bend, see Figure 3-5. The reduction in flow velocity at the patch seems to be determined by the meandering morphology. As meandering initiates secondary flow circulation near the apex, the flow moves relatively slow over the inner bank compared to the accelerated flow towards the outer bank (Blankeart and de Vriend, 2003; Furguson et al., 2003). The helix flow, which overflows the floodplain, is facing towards the vegetation patch at the apex at an angle, which initiates a higher blockage and therefore a higher resistance with lower flow velocities.

Multiple patches are also studied, which increase the velocity in patches nearby. The velocity increase in the patch induced by patches nearby is also found for experiments in tidal conditions (Temmerman et al, 2007) and in fluvial situations (Zong and Nepf, 2012). The increase of flow velocity at the edge for a single patch is reflected on the patch nearby, which therefore also has an increase in flow velocity. This could hinder further vegetation development and even cause uprooting of young vegetation stands. Furthermore, the flow velocity between the patches depends on the relative distance between them to the width of the patch (Vandenbruwaene et al., 2013). As patches are closer together, the patches will act as one and force the flow to go around, whereas a larger distance increases the flow velocity between the patches and stimulate channel development through the preferential flow path (Zong and Nepf, 2010; Vandenbruwaene et al., 2013). This distance relative to the widths of the patches is 0.7, which resulted in a small 9% decrease in flow velocity. Although other studies use a much smaller scale, Vandenbruwaene et al. (2013) shows that the patch start to act together at a ratio of inter patch distance relative to the patch width of 0.46-0.67, which is consistent with the vegetation patch modelling simulations.

4.2.2. REPRESENTATIVE REACH-SCALE CHÉZY

The blockage area by the vegetation is relatively small and the simulations represent blockages between 0% and 2%, which indicates a vegetated area of approximately 15% on the floodplain. Although this is realistic for a meandering river, other studies focus on the hydrodynamic response of vegetation patches in smaller streams with much higher blockage factors. These studies have blockage factors, up to 90%, to gain understanding of stream restoration to with the natural state, which is too high for flood conditions in a fluvial environment. Therefore, lower blockage factors better represent the natural state of the rivers. In order to make a comparison between the hydraulic response and the blockage, Green (2005a) and Nikora et al. (2008) relate the blockage to respectively a reach-averaged manning's and Chézy coefficient. The roughness coefficients proposed in these studies, which are based on their experimental simulations, would highly be overestimated for fluvial situations, as presented in this study. The correlation presented in Figure 4-1, for example, would result in variation of reach-averaged Chézy between 32.4 and 34.5 m$^{1/2}$/s. Smaller streams have relatively high velocities compared to the water depth, which result in these high Chézy's coefficients. The correlation of blockage by Green (2005a) to the manning's coefficient would even lead to an increase in Chézy relative to simulations without vegetation. However, the pattern of a decrease of the Chézy coefficient results to an increase of blockage is similar, although the simulations presented in this study are at a much larger scale.
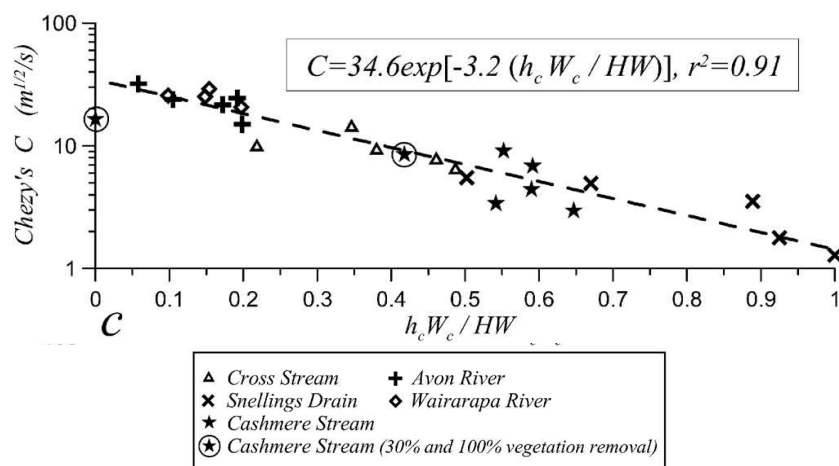

Figure 4-1 Correlation between blockage and the Chézy's coefficient for streams and small rivers highly overestimate Chézy's coefficient for a meander river. Furthermore, the resulting exponential pattern is hard to compare to this study, as the blockages are extremely high.

4.2.3. FLOW DIVERSION OVER THE FLOODPLAIN AND IN THE CHANNEL

The relative area of decelerated flow within the arc of the patch increases strongly for a patch position higher up the floodplain and is very low near the channel. So as the patch is closer to the channel, it stimulates the flow to take floodplain route and quicken the process of cutting off of meanders. As the patch moves higher up the floodplain, it closes of the floodplain and the area of deceleration behind the patch increases. This effect is stronger for taller vegetation. The redirection of the flow is studied for one shape of vegetation patch, although this vegetation pattern is very common in dynamic meandering systems, the leading edge could vary as a result of local events, such as wood logging. A different shape of patch could close off the floodplain more upstream, leading to different unknown flow field patterns and therefore a different flow diversion over the floodplain.

The added turbulences on the edges of multiple patches partly describe the unexplained variance in the relation between blockage and flow distribution between the channel and the floodplain. The flow between the patches is only partly blocked by the multiple patches and the relative velocity approaches one (0.91) which is close to the control situation. However, the flow at the leading edge and trailing edge show a much larger decrease and the multiple patches act together. Figure 4-1 supports the positive relation between the variance of the predicted flow distribution and the number of patches. Although the tall vegetation under high discharge conditions shows a negative trend, which remains unexplained.

5. CONCLUSION AND RECOMMENDATIONS

5.1. CONCLUSIONS

The conducted simulations in an idealized meandering planform illustrate the hydrodynamic response caused by the presence of a vegetation patch at a patch and river reach scale. The variation of the patch location and the number of patches give new insights in the water set-up in front of the patch, flow between vegetation patches and the general redirection of flow patterns on the floodplain induced by the blockage of the vegetation. This chapter presents an overview of the main findings in relation to the questions presented in section 1.5.

How does variation in the position of vegetation patches effect the raise in the water level within and near the vegetation patch?

- The location of the maximum water level does not change for the different positions of the vegetation patch and is located at the leading edge of the vegetation patch;
- The absolute raise in water level in the channel propagates more downstream near at the outerbank relative to the channel and this effect is stronger for vegetation patches closer to the channel.

How does variation in the position of vegetation patch redirect the velocity patterns within and near the vegetation patch?

- The relative flow deceleration in the vegetation patch depends only partly on the position of the vegetation patch, because the position controls the rate of submergence, as well as water level and the vegetation height, which determines the rate flow deceleration in the patch;
- The maximum relative deceleration of flow does not change for various position and is located just downstream of the apex, which is induced by the secondary flow patterns as a result of the meandering morphology;
- Vegetation patches closer to the channel increases flow velocities in the main channel;
- Patches higher up the floodplain discourage water flow over the floodplain, as the relative decelerated area in the arc increases.

How does variation in the numbers of vegetation patches raise the water level within and near the patches?

- The depression of water level behind and increase in water depth in front of the vegetation patches covers a larger area and is higher in magnitude for more vegetation patches;
- The relative velocity in downstream directed patches increase with more patches aligned parallel to the concerning patch.

How does variation in the vegetation patch number redirect the velocity patterns within and near the vegetation patch?

- The relative decelerated area in the arc decreases for more vegetation patches higher up the floodplain.

How does the blockage the various positions and the number of vegetation patches control the redistribution of discharge over the floodplain?

- The blockage factor, which covers the variation in water level, vegetation height, position and number of vegetation, explains most of the distribution over the floodplain and the channel at the apex.
- The interaction of flow in between the patches partly explains the variation between the blockage and the discharge distribution at the apex.

5.2. RECOMMENDATIONS

This section contains ideas for simulations based on a similar method, which are not executed in this study. The summery of the four recommended variations of variables is presented in Figure 5-1.

5.2.1. DISTANCE BETWEEN MULTIPLE PATCHES

Simulations in this study used a single distance (30m) between the patches relative to the width of the patch (20m). As the simulations in this study and previous studies showed, the variation of the blockage can partly be explained by the number of patches and this provides evidence that the flow between the vegetation interacts. Experiments in small scale streams with high blockages already studied the interaction of flow between patches for various distance, but the hydrodynamic effects in a large river system with associated morphology and a much lower relative blockage by vegetation is unknown. The results could support decisions of vegetation placement river managers.

5.2.2. SHAPE OF THE PATCH

Furthermore, the sensitivity on the redirection of flow by the shape of the patch entrance shape is unknown. This study simulates the hydrodynamic response for the same width over the whole patch alignment, as well as the entrance, although Figure 1-1D) shows various dimensions of entrances on the floodplain. This study presents strong redirection patterns as a result of the presence of the patch. The impact of a different entrance of vegetation patches is yet unidentified, although the distribution between channel and floodplain will vary for different types of entrances as our results showed that the location of the maximum water level increase is at the leading edge, which makes the shape of the entrance important for the flow alternation.

Secondly, the arc curvature of the patch varies for patches located in a meandering floodplain. As the meander evolves, new vegetation will follow the changing channel curvature and patches have a varying arc curvature depending on the distance to the channel. This study keeps the rate of curvature constant, although patches with a larger distance tend to have a lower curvature, as the river sinuosity is generally lower at the time of the establishment patch. Patches closer to the channel will follow the channel alignment, although during high flood events a higher curvature could imply a larger blockage as the high curvature patch is more perpendicular to the average flow direction.

5.2.3. DOWNSTREAM MIGRATION

A simplification of the downstream migration of the meander could be included as another exploration of the hydraulic effect within this systematic patch placement approach. Meander bend evolution generally comprises an increasing curvature and the downstream movement of the meander bend. The leading edge of the patch will end up closer to the channel, which shown in Figure 1-1D). The flow will be captured higher upstream and the hypothesis is that a larger portion flow will be redirected over the floodplain.
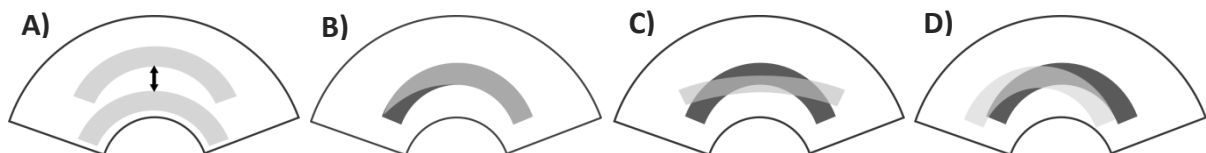

Figure 5-1 Overview of proposed changing variables to systematically determine the effect of vegetation patches on a meandering floodplain. Simulation with variations in A) the distance between the patches relative to the patch width, B) the shape of the leading edge, C) the degree of the arc of the patch and D) a simplification of the downstream migration of the meander bend.

6. ACKNOWLEDGEMENTS

7. REFERENCES

Abad J. D. and M. H. Garcia (2009), Experiments in a high-amplitude Kinoshita meandering channel: 1. Implications of bend orientation on mean and turbulent flow structure. *Water Resources Research, 45*(2), W02401.

Baptist, M.J., V. Babovic, J. Rodríguez Uthurburu, M. Keijzer, R. E. Uittenbogaard, A. Mynett and A. Verwey (2007), On inducing equations for vegetation resistance. *Journal of Hydraulic Research, 45*(4), 435–450.

Bendix, J. and C. R. Hupp (2000), Hydrological and geomorphological impacts on riparian plant communities. *Hydrological Processes 14*(16), 2977–2990.

Blanckaert, K. and H. J. De Vriend, (2003), Nonlinear modeling of mean flow redistribution in curved open channels. *Water Resources Research 39*(12), WR002068.

Bouma T. J., L. A. Van Duren, S. Temmerman, T. Claverie, A. Blanco-Garcia, T. Ysebaert and P. M. J. Herman (2007), Spatial flow and sedimentation patterns within patches of epibenthic structures: Combining field, flume and modelling experiments. *Continental Shelf Research 27*(8), 1020–1045.

Camporeale, C., E. Perucca and L. Ridolfi (2008), Significance of cutoff in meandering river dynamics. *Journal of Geophysical Research – Earth Surface 113*(F1), 001.

Choi S. U. and H. Kang (2004), Reynolds stress modeling of vegetated open-channel flows. *Journal of Hydraulic Research 42*(1), 3-11.

Corenblit, D., E. Tabacchi, J. Steiger and A. M. Gurnell (2007), Reciprocal interactions and adjustments between fluvial landforms and vegetation dynamics in river corridors: A review of complementary approaches. *Earth-Science Reviews 84*(1), 56–86.

Crosato, A. and E. Mosselman (2009), Simple physics-based predictor for the number of river bars and the transition between meandering and braiding. *Water Resources Research 45*(3), W03424.

Van Dijk, W. M. (2013), Meandering rivers- feedbacks between channel dynamics, floodplain and vegetation. *Utrecht Studies in Earth Sciences 035*.

Duel, H. and B. Specken (1994), Standplaatsmodel Wilgen-populierenbos: een model voor het analyseren van de standplaatskwaliteit van rivieroevers voor wilgen-populierenbossen *(Salicon albae)*, *TNO-BSA, Werkgroep Planning*, werkdocument 96.046x, Delft.

Eaton B.C. and M. Church (2007), Predicting downstream hydraulic geometry: A test of rational regime theory. *Journal of Geophysical Research - Earth Surface 112*(F3), 025.

Ferguson, R. I., D. R. Parsons, S. N. Lane and R. J. Hardy (2003), Flow in meander bends with recirculation at the inner bank, *Water resources research 39*(11), 1322.

Folkard, A. M. (2011), Flow regimes in gaps within stands of flexible vegetation: laboratory flume simulations. *Environmental Fluid Mechanics 11*(3), 289-306

Geerling, G. W., A. M. J. Ragas, R. S. E. W. Leuven, J. H., Berg, M. Breedveld, D. Liefhebber and A. J. M. Smits (2006), Succession and Rejuvenation in Floodplains along the River Allier (France). *Hydrobiologia 565*(1), 71–86.

Ghisalberti M. and H. Nepf (2009), Shallow flows over a permeable medium: The hydrodynamics of submerged aquatic canopies. *Transport in porous media 78*(2), 309-326.

Green, J. C. (2005a), Modelling flow resistance in vegetated streams: review and development of new theory. *Hydrological Processes 19*(6), 1245–1259.

Green J. C. (2005b), Comparison of blockage factors in modelling the resistance of channels containing submerged macrophytes. *River Research and Applications 21*(6), 671–86.

Gurnell A. M., T. D. Blackall and G. E. Petts (2008), Characteristics of freshly deposited sand and finer sediments along an island-braided, gravel-bed river: The roles of water, wind and trees. *Geomorphology 99*(1-4), 254-269.

Gurnell, A. M., W. Bertoldi and D. Corenblit (2012), Changing river channels: The roles of hydrological processes, plants and pioneer fluvial landforms in humid temperate, mixed load, gravel bed rivers. *Earth-Science Reviews 111*(1), 129–141.

Hughes, F. M. R. (1997), Floodplain biogeomorphology. *Progress in Physical Geography 21*(4), 501–529.

Hupp, C. R. and W. R. Osterkamp (1996), Riparian vegetation and fluvial geomorphic processes. *Geomorphology 14*(4), 277–295.

Huthoff, F. (2007), Modeling hydraulic resistance of floodplain vegetation. *UT Publications 58016.*

Järvelä, J. (2004), Determination of flow resistance caused by non-submerged woody vegetation. *Journal of River Basin Management 2*(1), 61–70.

Kinoshita, R. (1961), Investigation of channel deformation in Ishikari River. *Report to the Bureau of Resources, Ministry of Science and Technology of Japan,* 1-174.

Kleinhans, M. G. (2010), Sorting out river channel patterns. *Progress in Physical Geography 34*(3), 287–326.

Kleinhans, M. G. and J. H. Van den Berg (2011), River channel and bar patterns explained and predicted by an empirical and a physics-based method. *Earth Surface Processes and Landforms 36*(6), 721–738.

Klopstra, D., H. J. Barneveld, J. M. Van Noortwijk and E. H. Van Velzen (1997), Analytical model for hydraulic roughness of submerged vegetation. *Proceedings of the 27th IAHR Congress theme A Managing Water: Coping with Scarcity and Abundance*, San Francisco, 775-780.

Langbein, W. B. and L. B. Leopold (1966), River meanders, a theory of minimum variance. *U.S. Geological Survey Professional Papers 422*(H), 1-15.

Lesser, G. R., J. A. Roelvink, J. A. T. M. Van Kester and G. S. Stelling (2004), Development and validation of a three-dimensional morphological model. *Coastal Engineering 51*(8-9), 883-915.

Luhar M., J. Rominger and H. Nepf (2008), Interaction between flow, transport and vegetation spatial structure. *Environmental Fluid Mechanics 8*(5–6), 423–439.

Luhar M. and H. Nepf (2013), From the blade scale to the reach scale: A characterization of aquatic vegetative drag. *Advances in Water Resources 51*(1), 305–316.

Mahoney, J. M. and S. B. Rood (1998), Streamflow requirements for cottonwood seedling recruitment - an integrative model. *Wetlands 18*(4), 634–645.

Merigliano M. F. (2005), Cottonwood understory zonation and its relation to floodplain stratigraphy. *Wetlands 25*(2), 356–374.

Merritt, D. M., M. L. Scott, N. L. Poff, G. T. Auble and D. A. Lytle (2009), Theory, methods and tools for determining environmental flows for riparian vegetation: riparian vegetation-flow response guilds. *Freshwater Biology 55*(1), 206-255.

Nepf, H. M., (1999), Drag, turbulence, and diffusion in flow through emergent vegetation. *American Geophysical Union 35*(2), 79–489.

Nepf, H. M., (2012), Hydrodynamics of vegetated channels. *Journal of Hydraulic Research 50*(3), 37–41.

Nepf, H. M. and E. R. Vivoni (2012), Flow structure in depth-limited, vegetated flow. *Journal of Geophysical Research 105*(C12), 28,547-28,557.

Nicholas, A. P. (2013), Modelling the continuum of river channel patterns. *Earth Surface Processes and Landforms 39*(10), 1187-1196.

Nikora, V., S. Lamed, N. Nikora, K. Debnath, G. Cooper and M. Reid (2008), Hydraulic resistance due to aquatic vegetation in small streams: field study. *Journal of Hydraulic Engineering 134*(9), 1326–1332.

Nikuradse, J. (1930), Untersuchungen über turbulente Strömungen in nicht kreisförmigen Rohren. *Engineering Archive 1*(3), 306-322.

Parker, G. and E. D. Andrews (1986), On the time development of meanders bends. *Journal of Fluid Mechanics*, 162, 139-156.

Parker, G, P. R., Wilcock, C. Paola, W. E. Dietrich and J. Pitlick (2007), Physical basis for quasi-universal relations describing bankfull hydraulic geometry of single-thread gravel bed rivers. *Journal of Geophysical Research 112*(F4), 21.

Perucca, E, C. Camporeale and L. Ridolfi (2006), Influence of river meandering dynamics on riparian vegetation pattern formation. *Journal of Geophysical Research – Biosciences 111*(G1), 1–9.

Perucca, E, C. Camporeale and L. Ridolfi (2007), Significance of the riparian vegetation dynamics on meandering river morphodynamics. *Water Resources Research 43*(3), 1–10.

Schlichting, H. and K. Gersten (2000), Boundary Layer Theory (8th ed.). *New York: Springer*.

Schoelnyck J., T. De Groote, K. Bal, W. Vandenbruwaene, P. Meire and S. Temmerman (2011), Self-organised patchiness and scale-dependent bio-geomorphic feedbacks in aquatic river vegetation. *Ecography 35*(8), 760-768.

Seminara G., G. Zolezzi, M. Tubino and D. Zardi (2001), Downstream and upstream influence in river menadering. Part 2. Planimetric development. *Journal of Fluid Mechanics 438*(1), 213-230.

Siniscalchi, F., V. I. Nikora and J. Aberle (2012), Plant patch hydrodynamics in streams: Mean flow, turbulence and drag forces. *Water Resources Research 48*(1), W01513.

Van Splunder, I., H. Coops, L. A. C. J. Voesenek and C. W. P. M. Blom (1995), Establishment of alluvial forest species in floodplains: The role of dispersal timing, germination characteristics and water level fluctuations. *Acta botanica Neerlandica 44*(3), 269–278.

Spruyt A., E. Mosselman and B. Jagers (2011), A new approach to river bank retreat and advance in 2D numerical models in fluvial morphodynamics. *RCEM 2011: Proceedings of the 7th IAHR Symposium of River, Coastal and Estuarine Morphodynamics*, Beijing, China, 1863–1871.

Stella, J. C., M. K. Hayden, J. J. Battles, H. Piégay, S. Dufour and A. K. Fremier (2011), The Role of Abandoned Channels as Refugia for Sustaining Pioneer Riparian Forest Ecosystems. *Ecosystems 14*(5), 776–790.

Struiksma, N., K. W. Olesen, C. Flokstra and H. J. De Vriend (1985), Bed deformation in curved alluvial channels. *Journal of Hydraulic Research 23*(1), 57–79.

Sukhodolov A. N. and T. A. Sukhodolova (2010), Case Study: Effect of submerged aquatic plants on turbulence structure in a lowland river. *Journal of Hydraulic Engineering 136*(7), 434-446.

Tabacchi, E., D. L. Correl, R. Hauer, G. Pinay, A-M. Planty-Tabacchi and R. C. Wissmar (1998), Development, maintenance and role of riparian vegetation in the river landscape. *Freshwater Biology 40*(3), 497-516.

Talmon, A. M., N. Struiksma and M. C. L. M. Van Mierlo (1995), Laboratory measurements of the direction of sediment transport on transverse alluvial-bed slopes. *Journal of Hydraulic Research 33*(4), 495–517.

Temmerman, S., T. J. Bouma, J. Van de Koppel, D. Van der Wal, M. B. De Vries and P. M. J. Herman (2007), Vegetation causes channel erosion in a tidal landscape. *Geology 35*(7), 631-634

Vandenbruwaene W., S. Temmerman, T. J. Bouma, P. C. Klaassen, M. B. De Vries, D. P. Callaghan, P. Van Steeg, F. Dekker, L. A. van Duren, E. Martini, T. Balke, G. Bierman, J. Schoelynck and P. Meire (2011), Flow interaction with dynamic vegetation patches: Implications for biogeomorphic evolution of a tidal landscape. *Journal of Geophysical Reseach 116*(F01)*,* 088.

Vandenbruwaene W., T. J. Bouma, P. Meire and S. Temmerman (2013), Bio-geomorphic effects on tidal channel evolution: impact of vegetation establishment and tidal prism change. *Earth Surface Processes and Landforms 38*(2), 122-132.

Van Velzen, E. H., P. Jesse, P. Cornelissen and H. Coops (2002), Stromingsweerstand vegetatie in uiterwaarden. *Ministerie van Verkeer en Waterstaat, Rijkswaterstaat, Rijksinstituut voor Integraal Zoetwaterbeheer en Afvalwaterbehandeling (RWS, RIZA)*.

Vreugdenhil, S. J., K. Kramer and T. Pelsma (2006), Effects of flooding duration, -frequency, and –depth on the presence of saplings of six woody species in north-west Europe. *Forest Ecology and Management 236*(2-3), 47-55.

Yamaoka, I., and K. Hasagawa (1983), Effects of bends and alternating bars on meander evolution. *In River Meandering: Proceedings of the Conference River '83*, New York, 783–793.

Zong, L. and H. M. Nepf (2010), Flow and deposition in and around a finite patch of vegetation. *Geomorphology 116*(3-4), 363-372.

APPENDICES

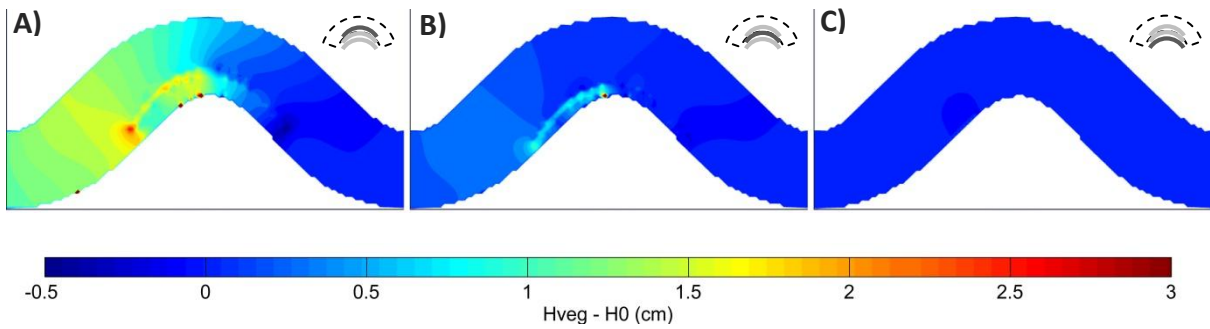# I.   CHANGES OF WATER LEVELS FOR ALL SIMULATIONS

Figure I-1 Water level changes for various positions of the vegetation patch on the floodplain for small vegetation with medium discharge conditions. The distance of the patch to the channel is A) 100m B) 150m and C) 200m.
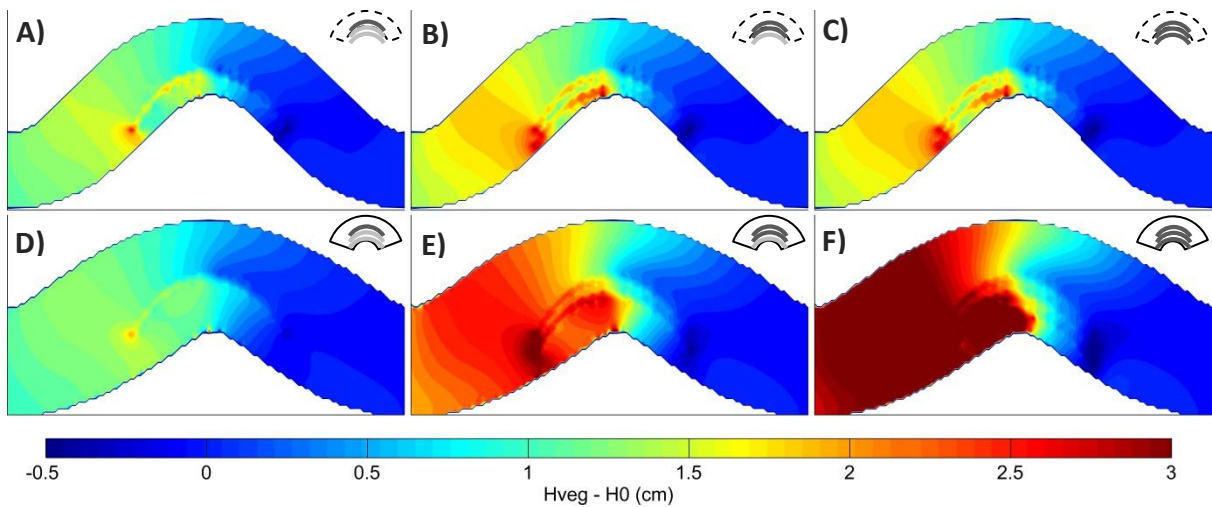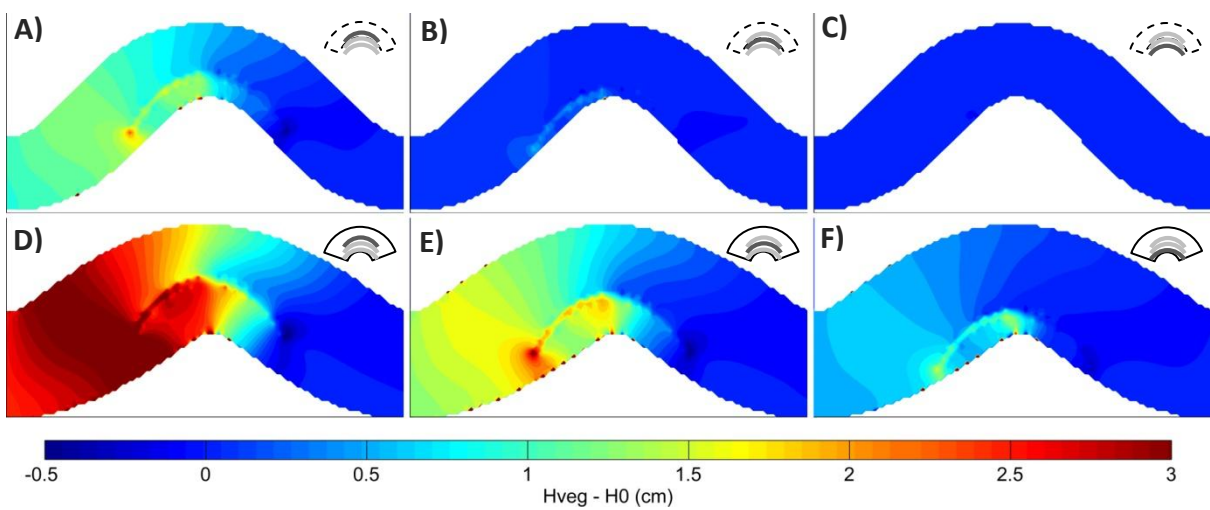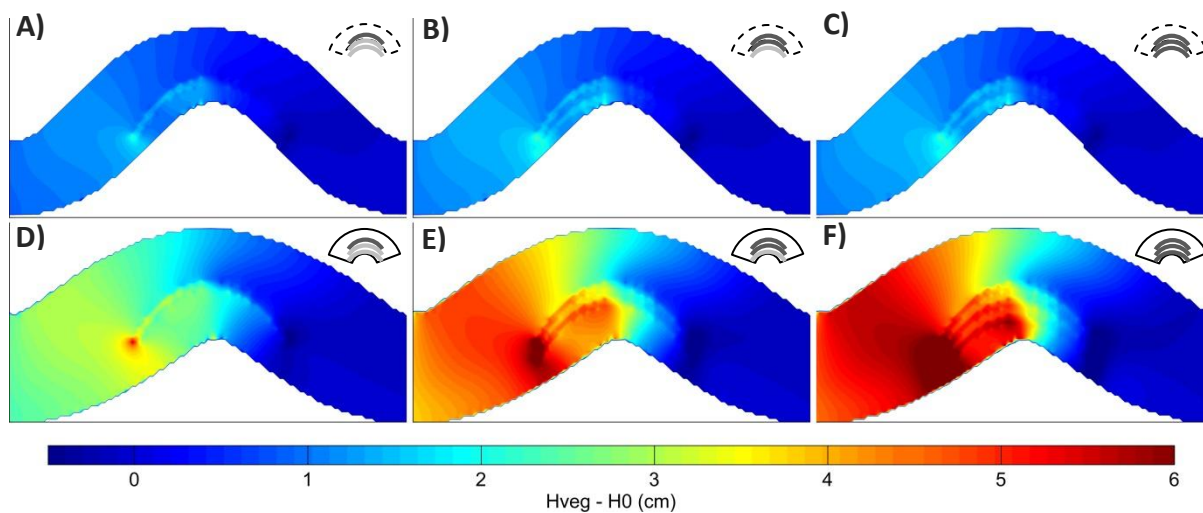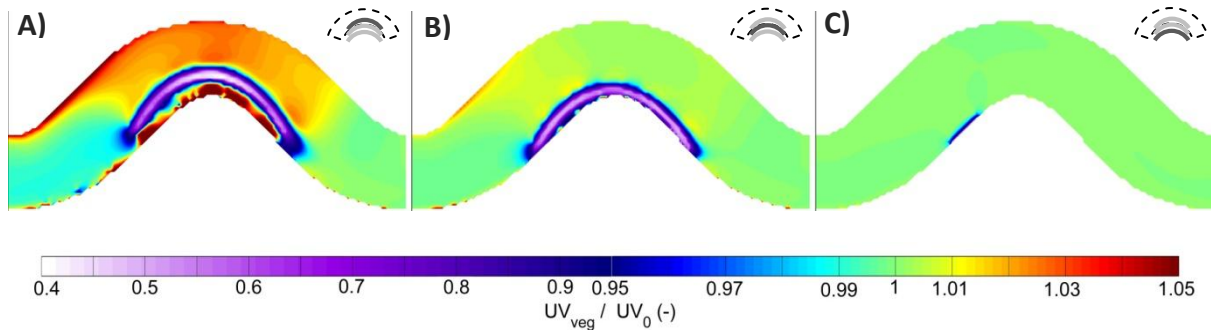

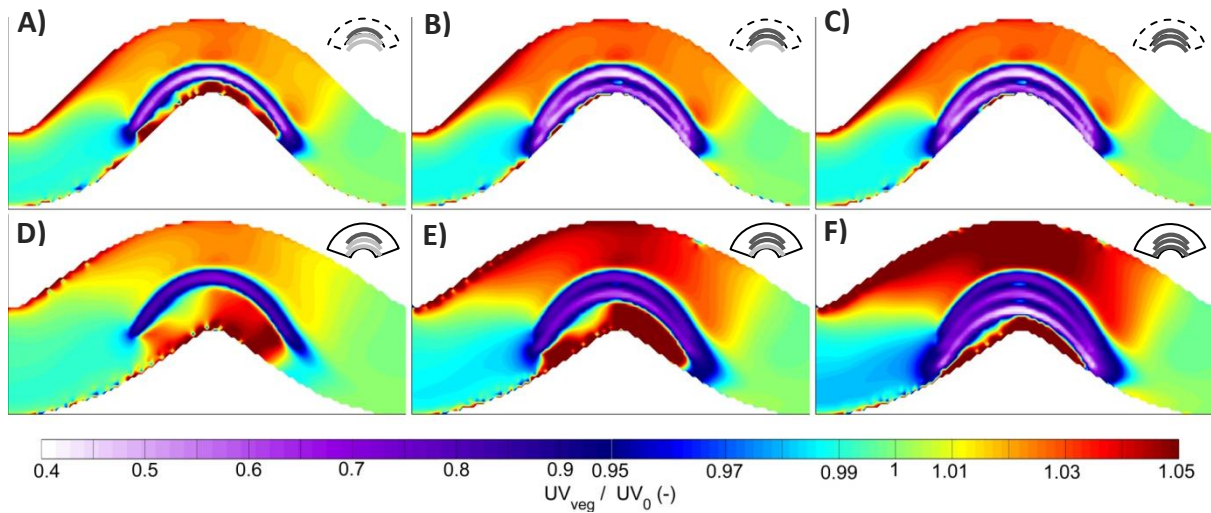**Figure I-2 Water level changes for a various number of the vegetation patches on the floodplain for small vegetation with medium and high discharge conditions. The distance to the channel is A) and D) 1 patch at 100m B) and E) 2 patches at 100m and 150m and C) and F) 3 patches at 100, 150 and 200m.**

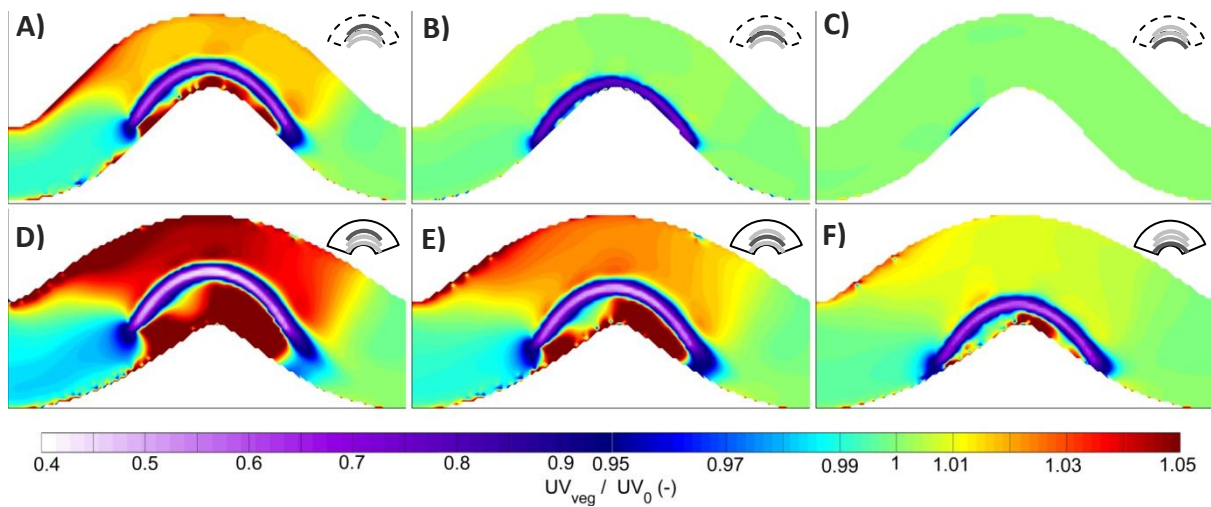**Figure I-3 Water level changes for various positions of the vegetation patch on the floodplain for large vegetation with medium and high discharge conditions. The distance of the patch to the channel is A) and D) 100m B) and E) 150m and C) and F) 200m.**

Figure I-4 Water level changes for a various number of the vegetation patches on the floodplain for large vegetation with medium and high discharge conditions. The distance to the channel is A) and D) 1 patch at 100m B) and E) 2 patches at 100m and 150m and C) and F) 3 patches at 100, 150 and 200m.

II. CHANGES OF THE MAGNITUDE OF THE VELOCITY FOR ALL SIMULATIONS

Figure II-1 Normalized velocity changes for various positions of the vegetation patch on the floodplain for small vegetation with medium discharge conditions. The distance of the patch to the channel is A) 100m B) 150m and C) 200m. Note the double linear scale bar.

Figure II-2 Normalized velocity changes for a various number of the vegetation patches on the floodplain for small vegetation with medium and high discharge conditions. The distance to the channel is A) and D) 1 patch at 100m B) and E) 2 patches at 100m and 150m and C) and F) 3 patches at 100, 150 and 200m. Note the double linear scale bar.

Figure II-3 Normalized velocity changes for various positions of the vegetation patch on the floodplain for large vegetation with medium and high discharge conditions. The distance of the patch to the channel is A) and D) 100m B) and E) 150m and C) and F) 200m. Note the double linear scale bar.
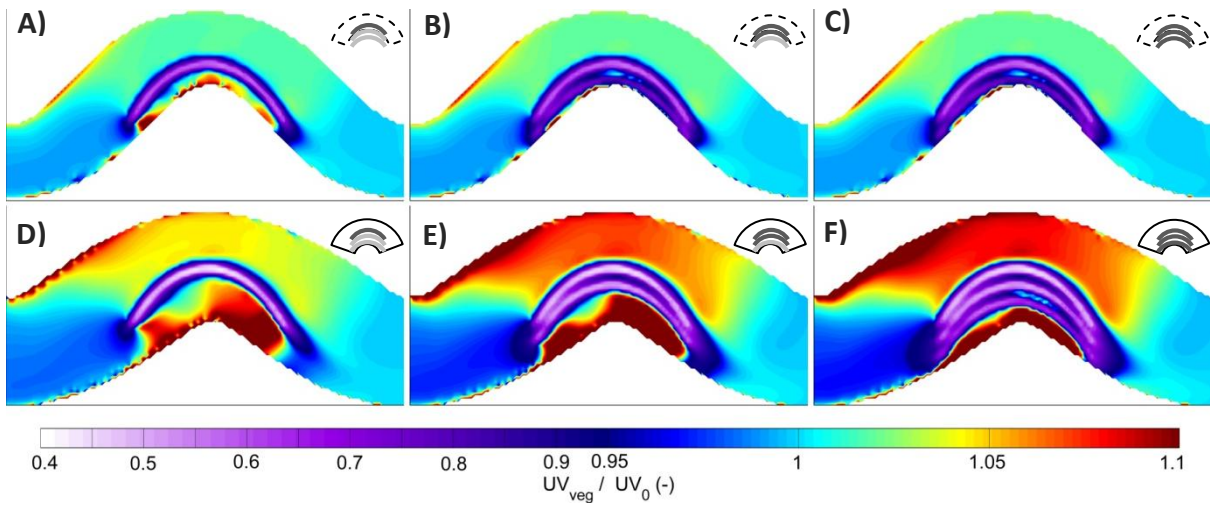
Figure II-4 Normalized velocity changes for a various number of the vegetation patches on the floodplain for large vegetation with medium and high discharge conditions. The distance to the channel is A) and D) 1 patch at 100m B) and E) 2 patches at 100m and 150m and C) and F) 3 patches at 100, 150 and 200m. Note the double linear scale bar.

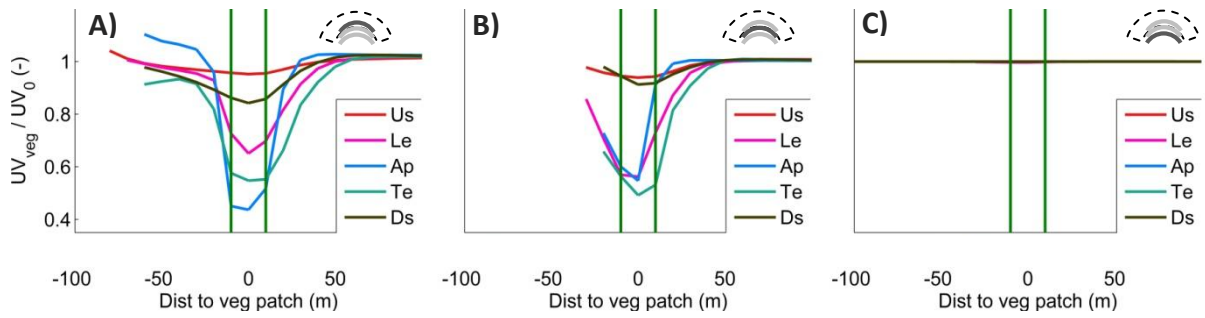# III. TRANSVERSE AND LONGITUDINAL PROFILES OF THE SIMULATIONS

Figure III-1 Transverse normalized velocity profiles for various positions of small vegetation patches. The green lines indicate the position of the vegetation and the coloured lines show the transeverse profiles of upstream (US), leading edge (le), Apex (ap), Trailing edge (TE) and downstream (Ds) of the vegetation.
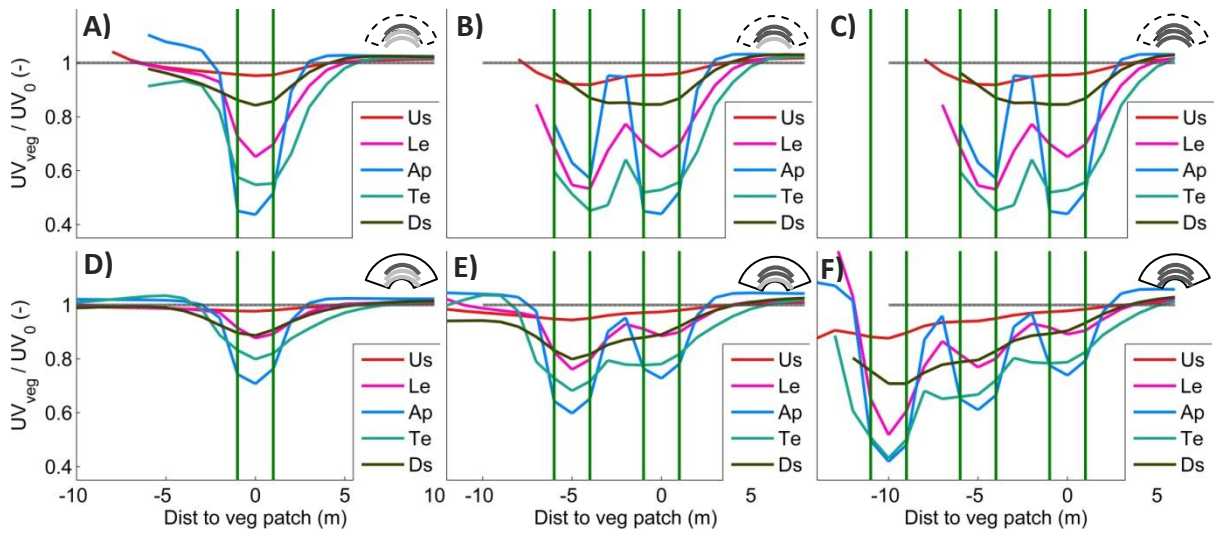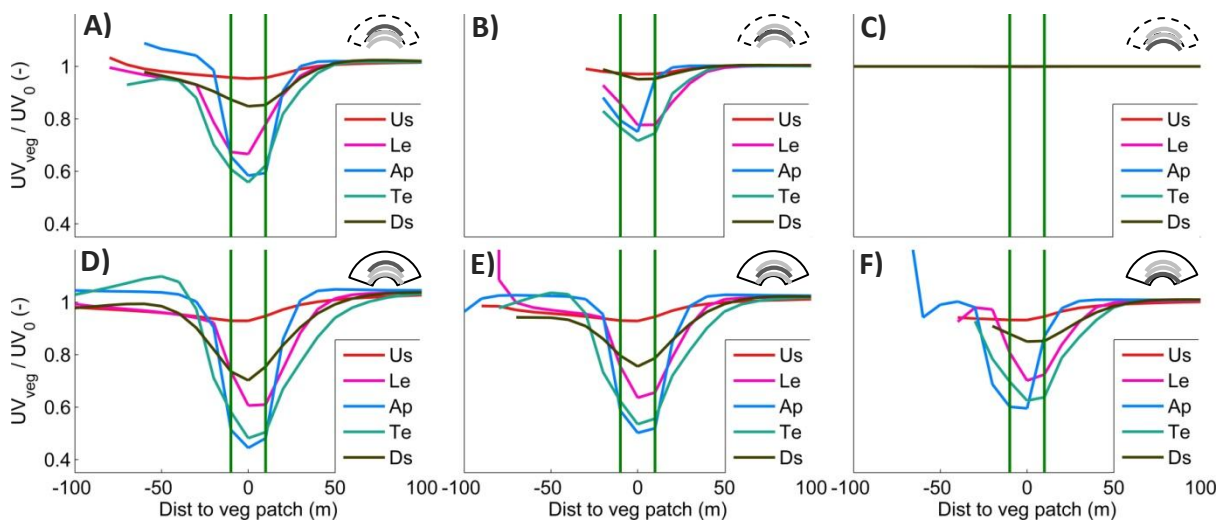

Figure III-2 Transverse normalized velocity profiles for a various number of vegetation patches of small vegetation. The green lines indicate the position of the vegetation and the coloured lines show the transeverse profiles of upstream (US), leading edge (le), Apex (ap), Trailing edge (TE) and downstream (Ds) of the vegetation.
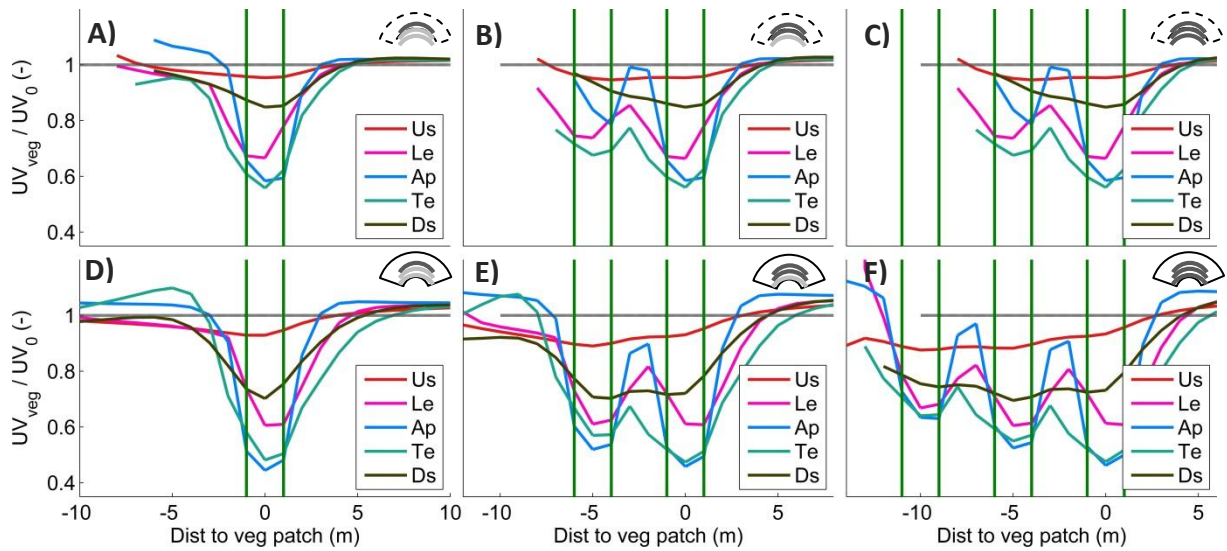

Figure III-3 Transverse normalized velocity profiles for various positions of large vegetation patches. The green lines indicate the position of the vegetation and the coloured lines show the transeverse profiles of upstream (US), leading edge (le), Apex (ap), Trailing edge (TE) and downstream (Ds) of the vegetation.
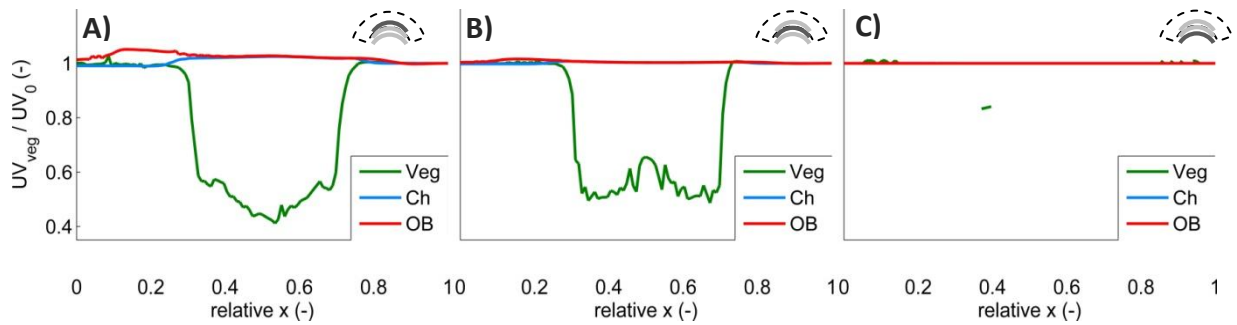
Figure III-4 Transverse normalized velocity profiles for a various number of vegetation patches of large vegetation. The green lines indicate the position of the vegetation and the coloured lines show the transeverse profiles of upstream (US), leading edge (le), Apex (ap), Trailing edge (TE) and downstream (Ds) of the vegetation.

Figure III-5 Longitudinal normalized velocity profiles for the various positions of the small vegetation patches for medium discharge conditions. The coloured lines show the longitudinal profiles of the vegetation, channel and outer bank.
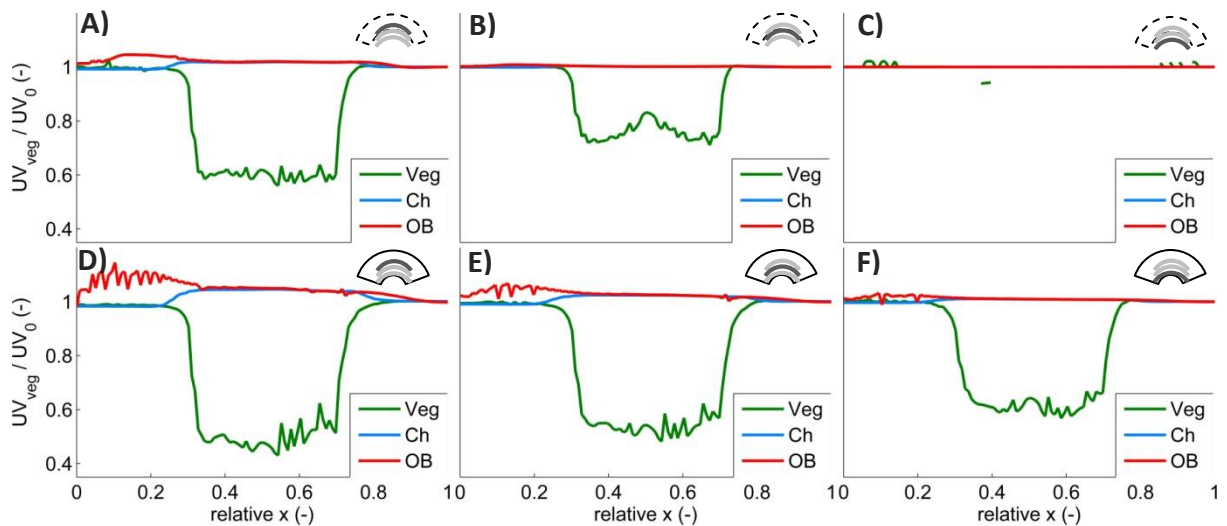

Figure III-6 Longitudinal normilized velocity profiles for the various positions of the vegetation patch of large vegetation for medium and high discharge conditions. The coloured lines show the longitudinal profiles of the vegetation, channel and outer bank.
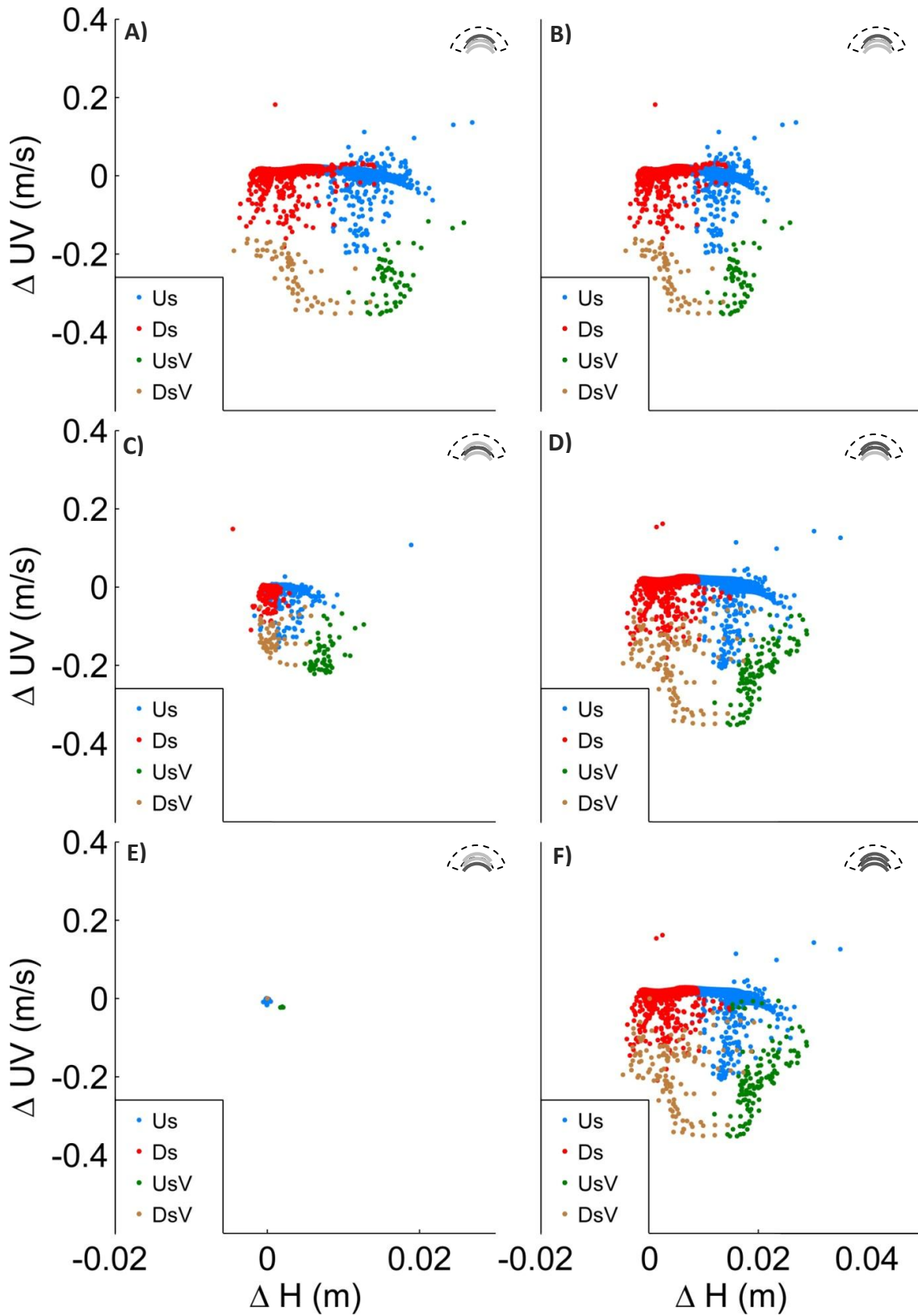
Figure IV-1 Water level and velocity changes for the six simulations for one meander wavelength for small vegetation and medium discharge conditions. The colour indicates the position on the meander reach: us = upstream of the apex, Ds = Downstream of the apex and V = vegetation.
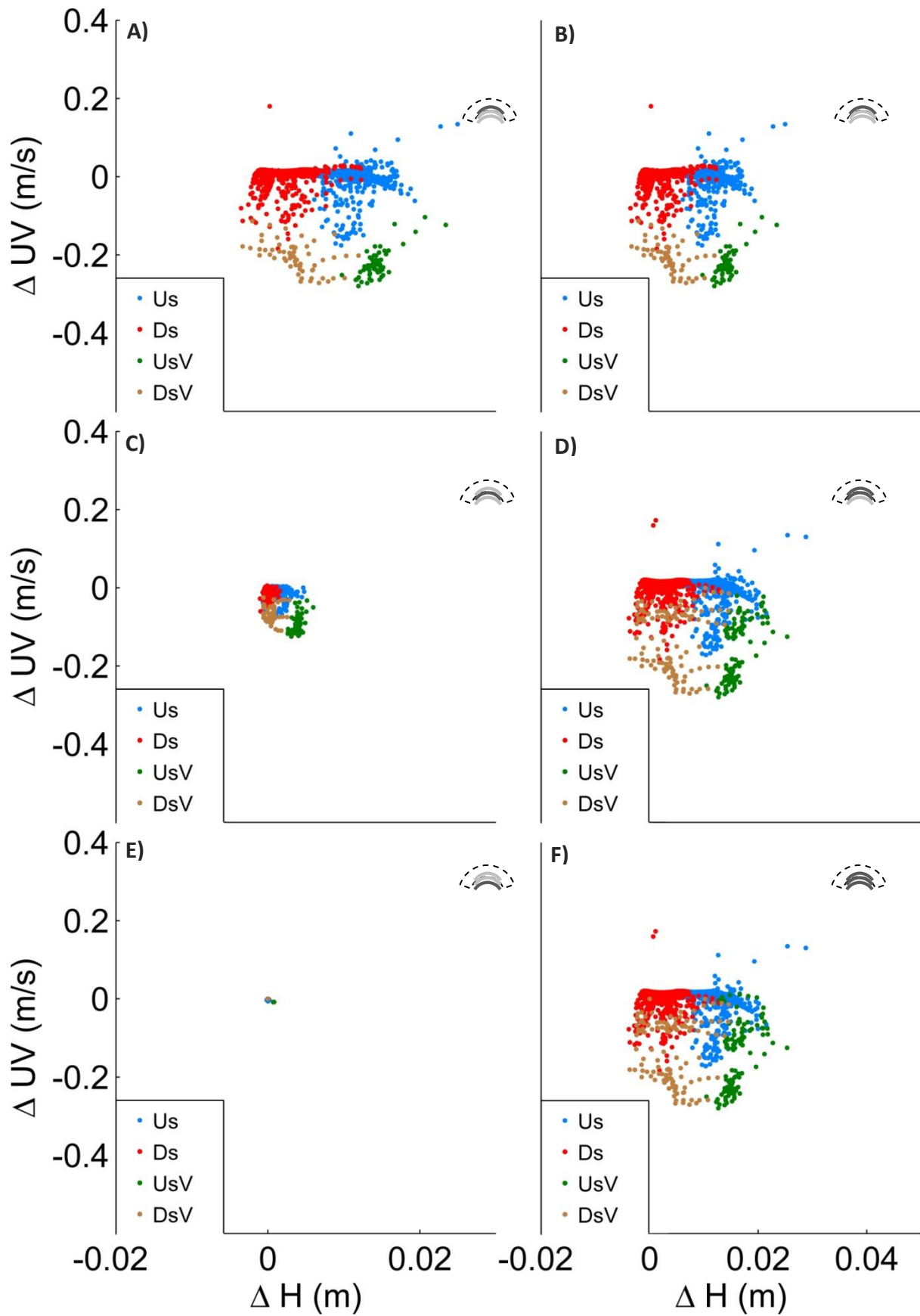
Figure IV-2 Water level and velocity changes for the six simulations for one meander wavelength for large vegetation and medium discharge conditions. The colour indicates the position on the meander reach: us = upstream of the apex, Ds = Downstream of the apex and V = vegetation.
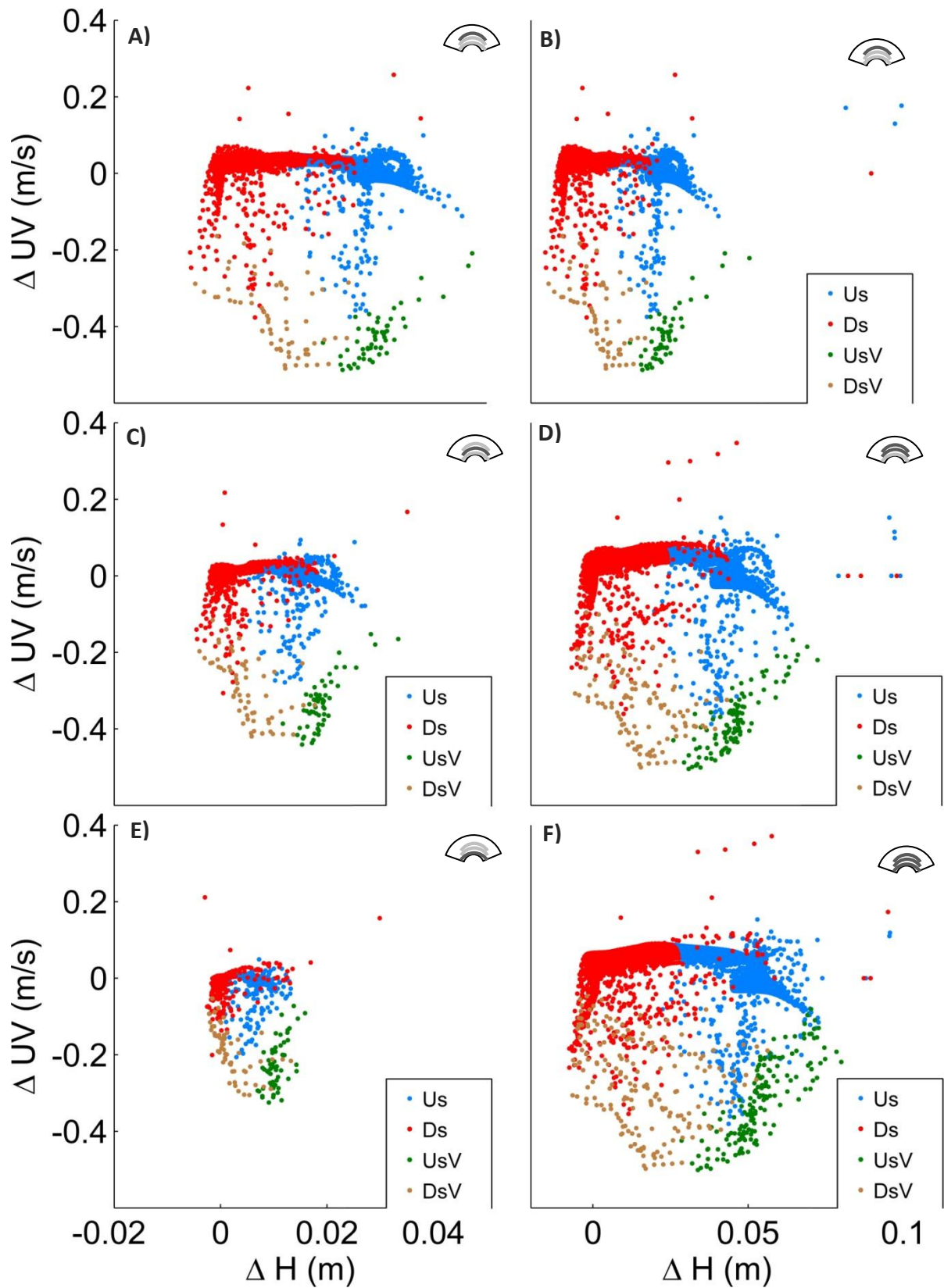
Figure IV-3 Water level and velocity changes for the six simulations for one meander wavelength for large vegetation and high discharge conditions. The colour indicates the position on the meander reach: us = upstream of the apex, Ds = Downstream of the apex and V = vegetation.

V.   Data structure

The hard disk contains the folder \Matlab with all relevant to do the whole process of making the bathymetry, place vegetation patches on the floodplain, run the Delft3D hydrodynamic module, gather data and visualize data. The folder \Results contains the data, to where the model simulations are exported. Lastly the folder \Thesis contains the end products of the master thesis. The full folder structure is presented in Figure V-1.
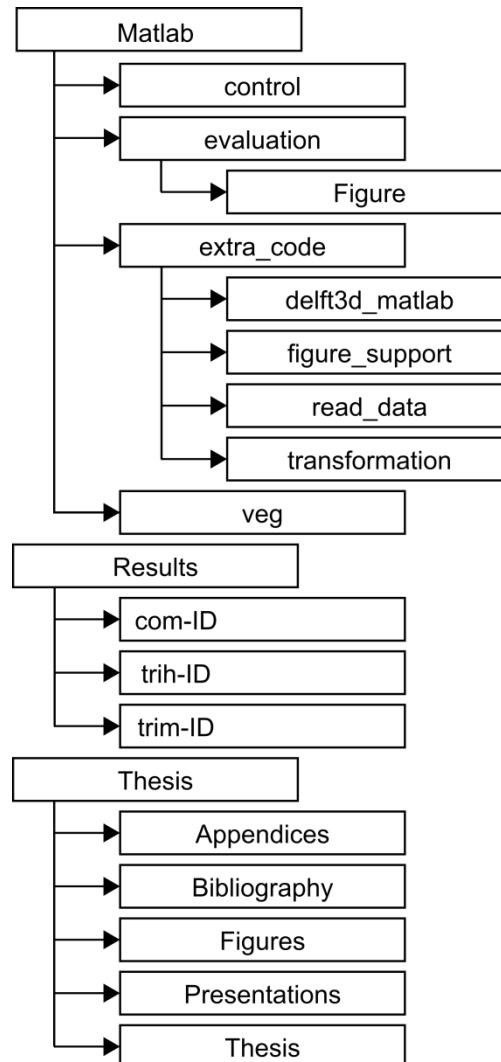

Figure V-1 The data structure of this thesis.

The two main Matlab codes for 1) developing the bathymetry and 2) initializing and executing the Delft3D code with various positions of vegetation patches are located in the \Matlab folder. After the execution of a simulation, the results are copied to the folder \Results, which store three types of files per simulation. The ID in Matlab coding style for every simulation is used for making executing the simulation, saving the results and accesses the results and if defined as follows:

```
ID=sprintf('rect_meander_%0.0f_%0.0f_%0.0f_%0.0f_%0.0f_%0.0f_%0
.0f_%0.0f',Q,veg,d,W_veg,shft,dist,nmb_pat,multi_pb);
```